The Invisible Hand Illusion: Multisensory Integration Leads to the Embodiment of a Discrete Volume of Empty Space

Arvid Guterstam, Giovanni Gentile, and H. Henrik Ehrsson

Abstract

■ The dynamic integration of signals from different sensory modalities plays a key role in bodily self-perception. When visual information is used in the multisensory process of localizing and identifying one's own limbs, the sight of a body part often plays a dominant role. For example, it has repeatedly been shown that a viewed object must resemble a humanoid body part to permit illusory self-attribution of that object. Here, we report a perceptual illusion that challenges these assumptions by demonstrating that healthy (nonamputated) individuals can refer somatic sensations to a discrete volume of empty space and experience having an invisible hand. In 10 behavioral and one fMRI experiment, we characterized the perceptual rules and multisensory brain mechanisms that produced this "invisible hand illusion." Our behavioral results showed that the illusion depends on visuotactile-proprioceptive integration that obeys key spatial and temporal multisensory rules confined to near-personal space. The fMRI results associate the illusion experience with increased activity in regions related to the integration of multisensory body-related signals, most notably the bilateral ventral premotor, intraparietal, and cerebellar cortices. We further showed that a stronger feeling of having an invisible hand is associated with a higher degree of effective connectivity between the intraparietal and ventral premotor cortices. These findings demonstrate that the integration of temporally and spatially congruent multisensory signals in a premotor-intraparietal circuit is sufficient to redefine the spatial boundaries of the bodily self, even when visual information directly contradicts the presence of a physical limb at the location of the perceived illusory hand. ■

INTRODUCTION

The problem of how the human brain identifies a body part as "self" represents a fundamental challenge in neuroscience and psychology. During the past decade, this question has become accessible to experimental investigation with the introduction of body illusions in which healthy participants experience dynamic changes in self-attribution and the spatial localization of their limbs (Moseley et al., 2008; Tsakiris & Haggard, 2005; Ehrsson, Spence, & Passingham, 2004; Botvinick & Cohen, 1998) and whole bodies (Petkova & Ehrsson, 2008; Ehrsson, 2007; Lenggenhager, Tadi, Metzinger, & Blanke, 2007). The first and most influential of these illusions is the rubber hand illusion (Botvinick & Cohen, 1998). In this experiment, the sight of a rubber hand being stroked by a paintbrush in synchrony with brushstrokes applied to one's hidden hand elicits an illusion that the touches are felt on the rubbery skin surface and that the rubber hand is part of one's own body. This illusion arises in the resolution of a multisensory conflict involving vision, touch, and proprioception, whereby somatosensory sensations become referred to the rubber hand. The existence of illusions that involve changes in the feeling of ownership of a body part supports the notion that the body is distinguished from other objects as belonging to the self by its nature of being the locus of specific multisensory perceptual correlations (Van den Bos & Jeannerod, 2002; Botvinick & Cohen, 1998; Rochat, 1998; Bahrick & Watson, 1985; Lewis & Brooks-Gunn, 1979). From a behavioral perspective, the construction and maintenance of a coherent internal representation of one's own body in space constitute an essential pre-requisite for our interactions with the external world (Graziano & Botvinick, 2002).

When vision is used, visual information related to the body itself often plays a dominant role in the process of localizing (Hagura et al., 2007; Clower et al., 1996; Van Beers, Sittig, & Denier van der Gon, 1996; Welch & Warren, 1986; Lackner & Taublieb, 1984; Welch, Widawski, Harrington, & Warren, 1979) and self-attributing (Tsakiris, Carpenter, James, & Fotopoulou, 2010; Petkova & Ehrsson, 2008) one's limbs in space. Specifically, studies on the rubber hand illusion have shown that a viewed object must resemble a human-like hand for the illusion to be elicited (Tsakiris et al., 2010; Haans, IJsselsteijn, & De Kort, 2008; IJsselsteijn, De Kort, & Haans, 2006; Tsakiris & Haggard, 2005). Accordingly, several models have proposed that a match between the visual form of a viewed hand-shaped object and implicit knowledge about the normal visual appearance of the

Karolinska Institutet, Stockholm, Sweden

doi:10.1162/jocn_a_00393

body is a *sine qua non* condition for inducing illusory hand ownership through synchronized visuotactile stimulation (Blanke, 2012; Ehrsson, 2012; Moseley, Gallace, & Spence, 2012; Tsakiris, 2010; Makin, Holmes, & Ehrsson, 2008). A further implicit assumption in the literature is that ownership sensations can be induced only for physical objects (in healthy nonamputated individuals). However, a recent pilot experiment in our laboratory put these assumptions into question by showing that it is possible to elicit an illusion of having an invisible hand that "feels" touches applied to it in empty space in direct view of the participants. To induce this "invisible hand illusion," a trained experimenter (AG) repetitively and synchronously applied brushstrokes to the participant's hand, which was hidden from view behind a screen, and to a portion of empty space in full view of the participant using an identical paintbrush. In this study, we characterized the perceptual rules and neural substrates of this illusion in 10 behavioral and one brain imaging experiment. Each experiment was designed to test a specific prediction related to the general hypothesis that the illusory experience of having an invisible hand is elicited by multisensory integrative mechanisms that operate in hand-centered spatial reference frames within perihand space (Ehrsson, 2012; Makin et al., 2008; see Table 1 for an overview and Methods and Results for details about each experiment). In line with this hypothesis, we found that the illusion obeys key temporal and spatial multisensory principles and is associated with the activation of a specific premotor-intraparietal circuit. These findings have implications for models of body ownership (Blanke, 2012; Ehrsson, 2012; Moseley et al., 2012; Tsakiris, 2010; Makin et al., 2008) because they inform us about the minimal conditions required for inducing illusory hand ownership through synchronized visuotactile stimulation. In fact, the invisible hand illusion demonstrates that the visuotactile integrative mechanisms involved in the self-attribution of a seen limb are, paradoxically, independent of the visual presence of a physical limb in the embodied volume of space.

METHODS

Participant Information

We recruited a total of 234 naive, healthy adult volunteers (of which 128 were female and 213 were right-handed) for the 10 behavioral experiments. No subjects participated in more than one experiment. For the final fMRI experiment, we selected 14 participants who had displayed a robust perceptual illusion in one of the questionnaire experiments (Experiments 1a–4a). Because the purpose of the fMRI experiment was to identify the neural correlates of the illusion, we considered it more important to ensure that the participants would actually experience the illusion inside the scanner than that they would be naive. These 14 participants were selected based on the following three average subjective rating inclusion criteria: (i) at least +2 on the test statements (T1–T2) for the illusion condition, (ii) less than −1 on the test statements (T1–T2) for the control condition, and (iii) less than −1 on the control statements (C1–C2) for all of the experimental conditions in the particular experiment they had participated in previously (see below for details concerning the questionnaires). The numbers of participants in each experiment are shown in Table 1. All participants gave written informed consent before participation, and the Regional Ethical Review Board of Stockholm approved all of the experimental procedures.

Table 1. Study Overview

Experiment	*Hypothesis Tested*	*Measure*	*N (Females)*	*Mean Age ± SD*
1a	Temporal congruency	Questionnaire	20 (10)	26 ± 6.5
1b	Temporal congruency	SCR	34 (18)	27 ± 7.7
1c	Temporal congruency	Proprioceptive drift	20 (11)	25 ± 5.8
2a	Spatial reference frames	Questionnaire	20 (13)	28 ± 8.6
2b	Spatial reference frames	SCR	28 (13)	28 ± 12.3
3a	Within/outside reaching space	Questionnaire	20 (12)	26 ± 8.3
3b	Within/outside reaching space	SCR	22 (15)	27 ± 8.2
4a	Empty space versus an object	Questionnaire	20 (13)	28 ± 5.0
4b	Empty space versus an object	SCR	30 (17)	29 ± 9.8
5	Neural mechanisms	fMRI	14 (6)	26 ± 5.1
Pilot[a]	Versus rubber hand illusion	Questionnaire	20 (9)	25 ± 4.5
		Total number of naive participants:	234	

[a]Data not shown.

Table 2. Questionnaire Statements Used in Experiments 1a–4a

	During the Experiment …
T1	… I felt the touch of the brush in empty space in the location where I saw the brush moving.
	… I felt the touch of the brush on the block of wood.[a]
T2[b]	… it felt as if my right hand were located on the table where I saw the brush moving, as if I had an "invisible" hand.[c]
	… I felt as if the block of wood were part of my body.[a]
C1	… I felt the touch of the brush directly on the table below where I saw the brush moving.
	… it appeared (visually) as if the block of wood were drifting to the right (toward my real arm).[a]
C2	… it felt as if my right hand disappeared, as if it had been "amputated."
	… it felt as if my right hand were located "inside" the rubber stump.[d]
	… it felt as if my (real) right hand were turning "wooden."[a]

The test statements (T1–T2) were designed to capture the subjective experience of the illusion, whereas the control statements (C1–C2) served as controls for suggestibility and task compliance.

[a]The questionnaire used for the block of wood condition in Experiment 4.

[b]After the conditions in which a rubber stump was used (Experiments 1 and 4), T2 stated, "It felt as if my right hand were located in front of the rubber stump…."

[c]The questionnaire of Experiment 4 used the term "invisible arm" instead of "invisible hand" for the "no rubber stump" condition.

[d]The questionnaire used after the conditions in which a rubber stump was used.

Behavioral Experiments

All of the behavioral experiments followed the same general structure and consisted of a 1-min period in which touches were delivered to the real right hand and invisible hand. After each stimulation period, we quantified the illusion using questionnaire reports in the form of visual analogue scale ratings of different statements (Experiments 1a–4a; see Table 2 for the statements), physiological evidence obtained by registering skin conductance responses (SCR) when threatening the invisible hand with a knife (Experiments 1b–4b) or the degree of pointing error toward the invisible hand (proprioceptive drift) in an intermanual pointing task in which participants (blindfolded) were asked to indicate the position of their right index finger using their left hand (Experiment 1c).

Experimental Setup and Illusion Induction Procedure

The experiments took place in a soundproof testing room (40-dB noise reduction). The participants sat on a comfortable chair and rested their arms on a table in front of them. The participants' right arm was placed behind a screen (for all the experiments except in Experiment 2a, where the arm was placed below a small table) and was thus hidden from view in all experiments. The experimenter sat opposite the participant.

The illusion was induced by applying brushstrokes to the participant's hidden real hand and simultaneously moving another paintbrush 1–5 cm above the table (depending on the size and posture of the participant's real hand) in the empty space to the left of the screen, which was in full view of the participant. A trained experimenter (AG) moved the paintbrush in the empty space in a manner that reflected the exact movements of the brush touching the real hand, following the shape of the knuckles and angles of the finger phalanges, as if it were touching an identical invisible right hand. We carefully matched the velocity, frequency, and skin surface stimulated by the brushstrokes across conditions in all of the experiments. The strokes were applied to all five fingers of the participant's right hand and corresponding locations on the "invisible hand." The strokes consisted of long strokes (along the entire length of the finger), short strokes (along the length of one finger phalange), and short tapping movements on the knuckles and fingernails. The tapping movements were not performed in Experiments 2 and 5, because there were conditions in these experiments in which the direction of the brush strokes was manipulated. The distance between the index finger of the participant's right hand and the index finger of the invisible hand was 20 cm (the only exception was in Experiment 2a, in which the invisible hand was displaced 15 cm vertically as a part of the specific experimental design; see below).

The first 10 sec of stroking were slightly different in the experiments that included illusion conditions in which a rubber stump was used (i.e., Experiments 1 and 4 and the pilot). The experimenter began by stroking the rubber stump (and the corresponding skin surface on the participant's forearm) for a period of 10 sec and then performed one very long stroke starting at the rubber stump and continuing over the edge into the empty space in front of the rubber stump, where the invisible hand was "located." To

maintain constant visual and tactile input across the conditions within the experiment, brushstrokes were delivered in a similar manner in conditions where no rubber stump was present or when a block of wood was used.

In the illusion condition, we used an irregular but synchronous brushing rhythm. In the asynchronous control condition, the pattern of brushing was irregular and alternated between the real hand and the invisible hand, which is an established method that significantly reduces the rubber hand illusion and permits the comparison of otherwise equivalent conditions (Tsakiris & Haggard, 2005; Ehrsson et al., 2004; Botvinick & Cohen, 1998). Approximately 30 strokes were applied per minute. In all conditions, the participants were instructed to look at the tip of the moving paintbrush throughout the stimulation session.

Questionnaires: Subjective Measurement of the Illusion

To quantify the subjective experiences associated with the illusion, we used questionnaires that were presented at the end of each condition (Botvinick & Cohen, 1998). The participants were then asked to affirm or deny different statements reflecting potential perceptual effects using a 7-point visual analogue scale that ranged from −3 to +3. The participants were informed that −3 indicated "*I completely disagree*," +3 indicated "*I agree completely*," and 0 indicated "*I do not know, I can neither agree nor disagree*." Test statements 1 and 2 (T1–T2) were used to examine the key perceptual components of the illusion, and Control statements 1 and 2 (C1–C2) were used as controls for suggestibility and task compliance. Table 2 summarizes the different statements used in all of the experiments. The formulation varied slightly between experiments according to the different styles of brushing during the initial 10 sec, the presence of a rubber stump, and the conditions in which blocks of wood were used.

SCR and Knife-threat Procedure: Objective Physiological Measures of the Illusion

We physically "threatened" the perceived invisible hand with a knife and measured the brief evoked increases in skin conductance to provide objective evidence for the illusion. In the context of well-controlled perceptual illusion paradigms, the SCR is a reliable index of the feeling of body ownership (Guterstam & Ehrsson, 2012; Guterstam, Petkova, & Ehrsson, 2011; Petkova & Ehrsson, 2009; Ehrsson, Wiech, Weiskopf, Dolan, & Passingham, 2007; Armel & Ramachandran, 2003). We balanced the stimulation order and included appropriate control conditions; therefore, we could relate changes in the SCR to changes in illusory ownership and exclude more general factors, such as surprise, general arousal, or nonspecific emotional responses related to the presentation of the knife. The SCR was recorded with a Biopac System MP150 (Goleta, USA) following standard published guidelines (Dawson, Schell, & Filion, 2007).

In this study, the threat stimulus consisted of stabbing the invisible hand with a knife after a period of repeated stroking of the participant's right hand and the empty space "occupied" by the invisible hand. The experimenter moved a small kitchen knife (22 cm long) toward the invisible hand in a motion that mimicked stabbing the hand at the level of the metacarpophalangeal joint. Importantly, the experimenter avoided any knife movements that could be perceived as threatening to the participant's thorax, face region, or real right hand hidden behind the screen. Accordingly, the knife approached the invisible hand at a 20–25° downward trajectory from the participant's left side (along the horizontal axis from the participant's point of view) and stopped after "hitting" the invisible hand (in Experiment 4b, the knife movement stopped just before "hitting" the invisible hand or block of wood). Next, the knife disappeared from the subject's field of view as the experimenter slid the knife in a motion away from the participant (along the sagittal axis from the participant's point of view). The visible movement of the knife was performed over approximately 2 sec. Care was taken to perform the same movements with the knife from trial to trial, that is, controlling the velocity and acceleration of the movement. Before the experiments commenced, all participants were shown one example of a knife threat to ensure that the procedure was not perceived as too frightening and to reduce any effect on the SCR that was related to seeing the knife for the first time. Participants were also instructed to shift their attention from the paintbrush moving in the empty space to the knife as soon as it was presented to ensure that they perceived the threat. In all of the SCR experiments, each experimental condition was repeated three times, and between each period of stroking, there was a 1-min resting period.

The threat-evoked SCR was identified as the peak of the conductance that occurred within 5 sec of the onset of the threat stimulus (from the first moment that the knife entered the participant's visual field) and was flagged in the SCR recording file. The amplitude of the SCR was calculated as the difference between the maximum and minimum values of the identified response. The investigator performing the analysis was blind to the condition (i.e., illusion or control). The average of all responses for each participant, including those in which no increase in amplitude was apparent, was separately calculated for each condition, and this value was taken as the SCR magnitude (Dawson et al., 2007). Thereafter, the SCR magnitudes for all the participants were compared statistically across different conditions as described in the Results section. The participants who did not display any threat-evoked SCR in at least 50% of the trials were considered nonresponders and excluded from the analysis (Guterstam et al., 2011; Petkova & Ehrsson, 2008). Thirty-eight participants (25% of all the total number of participants) were nonresponders. These participants are not included in Table 1.

Proprioceptive Drift: Objective Behavioral Measurement of the Illusion

The classical rubber hand illusion is associated with a drift in the perceived location of the hand toward the location of the rubber hand (Tsakiris & Haggard, 2005; Botvinick & Cohen, 1998). Moreover, a higher proprioceptive drift is associated with a higher rating of the feeling of ownership for the observed hand (Tsakiris & Haggard, 2005; Botvinick & Cohen, 1998; but see Rohde, Di Luca, & Ernst, 2011, for a critical view). To provide additional objective behavioral evidence for the invisible hand illusion, we registered the proprioceptive drift in Experiment 1c (and in the postscan behavioral experiment, see corresponding section below). For Experiments 2–4, we chose to use only one objective behavioral measure for the illusion. Because there is a well-documented positive correlation between the ownership sensation of an artificial hand and threat-evoked neuronal responses in areas related to anxiety (Ehrsson et al., 2007), we decided to use the SCR and not the proprioceptive drift.

Each experimental condition was repeated three times. Between each period of stroking, there was a resting period of 1 min. Immediately before and after each period of brushing, the participants were asked to close their eyes and indicate the position of their right index finger by pointing with their left hand. Before obtaining this response, the experimenter placed the participant's left index finger at one of three fixed starting points (the starting points were different for each repetition of a given condition and the order was balanced across participants) on a 1-m-long metal ruler (the ruler's markings were only visible to the experimenter) positioned 32 cm above the table and 49 cm in front of the participant's body. Next, the experimenter asked the participants to move their finger briskly along the ruler (which contained a shallow groove) and stop when the finger was immediately above where they felt the right index finger was located. We computed the differences in the pointing error (toward the invisible hand) between the measurements obtained before and after each stimulation period. The average of these differences was compared between the two conditions using a paired *t* test (Experiment 1c).

Experimental Design: Rationale and Conditions

Experiment 1a–c: Temporal Visuotactile Congruency Necessary for the Illusion

The aim of Experiment 1 was to provide subjective and objective evidence for the invisible hand illusion. Specifically, we tested our prediction that the elicitation of the illusion depends on the temporal synchrony of the visual brush movements in empty space and the tactile stimulation of the real hand because this multisensory principle is crucial for inducing many perceptual body illusions (Petkova & Ehrsson, 2008; Ehrsson, 2007; Lenggenhager et al., 2007; Botvinick & Cohen, 1998). Therefore, in three separate experiments, we combined the questionnaire (Experiment 1a), SCR (Experiment 1b) and proprioceptive drift (Experiment 1c) measurements using two experimental conditions: synchronous (illusion condition) and asynchronous stroking (control condition) of the participant's real and invisible hands. In these experiments (1a–c), a rubber stump that the experimenter began brushing before continuing to the invisible hand was always present (see Experimental setup above and Figure 1A).

Experiment 2a–b: Congruent Visuotactile Stimulation in Hand-centered Reference Frames Crucial for the Illusion

Experiment 2 tested the hypothesis that the integration of visuotactile signals that leads to the sense of having an invisible hand takes into account the proprioceptive information essential to define a hand-centered spatial reference frame (Costantini & Haggard, 2007). This hypothesis is consistent with the notion that the illusion is induced by visuotactile-proprioceptive integration mechanisms that operate in a hand-centered reference frame within peripersonal space (Brozzoli, Gentile, & Ehrsson, 2012; Ehrsson, 2012; Brozzoli, Gentile, Petkova, & Ehrsson, 2011; Makin

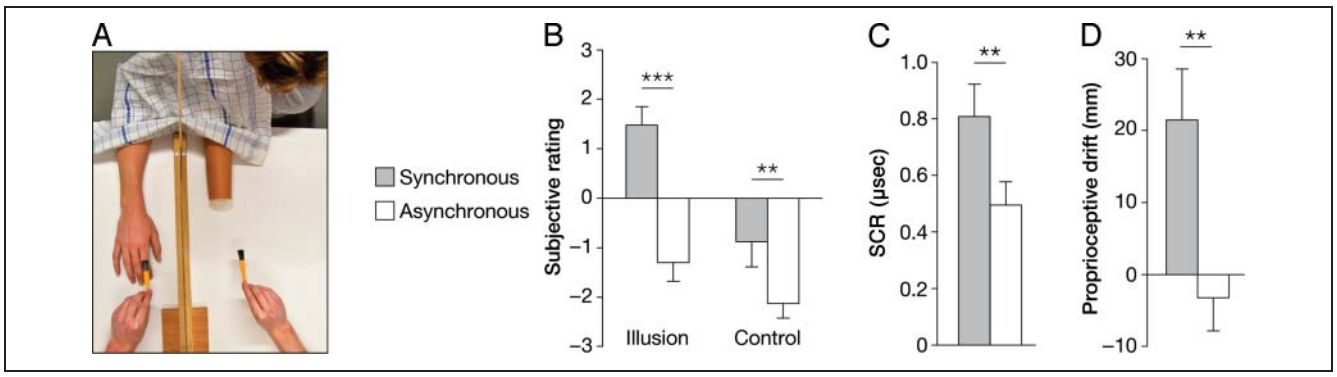

Figure 1. Experiment 1: Temporal congruency. (A) Experimental setup for Experiments 1a–c. (B) Experiment 1a: Average ratings of the statements in the questionnaire that reflected the illusory percept (test statements T1–T2) and the control statements (C1–C2). (C) Experiment 1b: Mean threat-evoked SCR. (D) Experiment 1c: Mean proprioceptive drift toward the location of the invisible hand. The error bars denote *SEM*.

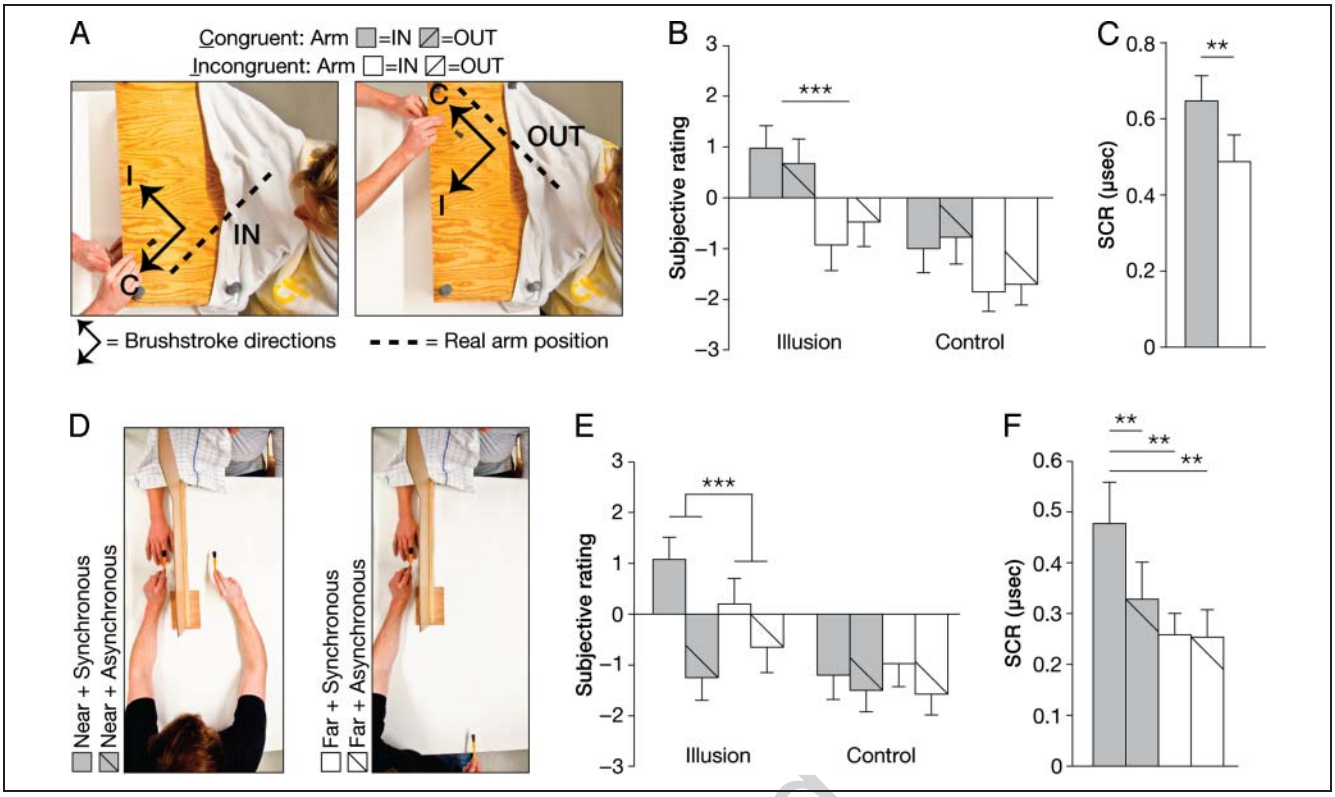

Figure 2. Experiments 2–3: Spatial congruency and reference frames. (A) Experimental setup for Experiments 2a and b. (B) Experiment 2a: Average ratings of the illusion statements (T1–T2) and control statements (C1–C2). (C) Experiment 2b: Mean threat-evoked SCR. (D) Experimental setup for Experiment 3a–b. (E) Experiment 3a: Average ratings of the illusion (T1–T2) and control statements (C1–C2). (F) Experiment 3b: Mean threat-evoked SCR. The error bars denote *SEM*.

et al., 2008). Thus, we independently manipulated two factors: arm posture and brushstroke direction. In Experiment 2a, the participant's right arm was hidden below a small 15-cm-high table. The arm was placed in one of two positions, "arm_{IN}" or "arm_{OUT}," that differed by 90° in the angle of forearm orientation (Figure 2A). The brushing was always applied synchronously to the hidden real hand and a volume of empty space that represented the invisible hand directly above the top of the small table (notably, in this and the subsequent experiments, the rubber stump was left out). The brushstrokes on the invisible hand were applied in two directions with a 90° angle between the two stroke trajectories. The direction of these strokes was congruent or incongruent with respect to the position of the hidden real arm (which was always stroked along the direction of the fingers). Thus, there were four different conditions. In the Arm_{IN} + $Brush_{IN}$ and Arm_{OUT} + $Brush_{OUT}$ illusion conditions, the anatomical arm position and observed brushstroke direction were *congruent* in a hand-centered frame of reference; in the Arm_{IN} + $Brush_{OUT}$ and Arm_{OUT} + $Brush_{IN}$ control conditions, the arm position and brushing direction were *incongruent* in hand-centered reference frames. We hypothesized that the invisible hand illusion would be exclusively elicited in the *congruent* conditions; that is, we expected to elicit the illusion for both arm postures but only when the direction of the brushstrokes in the empty space was iso-directional with the direction of the strokes applied to the arm.

In the questionnaire experiment (Experiment 2a), we included all four of the conditions mentioned above. To minimize habituation effects in the SCR recordings arising from repeated threat procedures and to increase the statistical power in Experiment 2b, we limited the experiment to two conditions: synchronous congruent or incongruent brushing of the real hand and invisible hand. Here the real arm was hidden behind a screen (as in Experiment 1) and was always in the same anatomical position; however, the visible brush strokes were spatially aligned with the tactile stimulations on the real hand ("congruent") or rotated by 90° ("incongruent," that is, the brush was moved along the horizontal axis, from the participant's point of view, in the direction away from the screen).

Experiment 3a–b: Invisible Hand Illusion Restricted to Near-personal Space

The aim of Experiment 3 was to examine whether the neuronal processes that produced the sensation of having an invisible hand were restricted to visual stimulation within the space close to the body, which may be referred to as near-personal or peripersonal space (Brozzoli et al., 2011; Làdavas & Farnè, 2004; Maravita, Spence, & Driver,

2003; Graziano, 1999, 2000). Work on the rubber hand illusion has demonstrated that the rubber hand must be placed within reaching distance from the real hand for the illusion to occur (Lloyd, 2007), which could reflect the response properties of visuotactile bimodal neurons that encode the peripersonal space around the hand (Graziano, Hu, & Gross, 1997a). Thus, we hypothesized that the invisible hand illusion would be restricted to the limits of reaching space. In this experiment, the visual stimulation of the invisible hand parallel to the real hand was performed within the participant's reaching space ("near" condition) or outside the limit of the participant's reach (75 cm in front of the participant's real hand) in the far extrapersonal space ("far" condition) as shown in Figure 2D. To control for potential differences in the threat-evoked SCR arising from the visual impressions of seeing a knife at different distances from the eyes, we included asynchronous control conditions for the far and near positions and employed a 2 × 2 factorial design (distance and timing). Thus, there were four conditions: *near-sync* (illusion condition), *near-async*, *far-sync*, and *far-async* (control conditions). The inclusion of the asynchronous control condition at the near location also allowed us to replicate the results of Experiment 1a–b using an invisible hand condition without using a rubber stump (i.e., the contrast of the *near-sync* and *near-async* conditions), which further strengthens the conclusion that the illusion can be efficiently induced without a stump.

Experiment 4a–b: The Invisible Hand versus a Block of Wood; The Invisible Hand with or without a Stump

The aim of Experiment 4 was twofold. First, we tested the hypothesis that the illusion would be specific to congruent visuotactile stimulation in the empty space and that it would not work with a neutral object presented in front of the participants. Thus, we defined a control condition in which a block of wood was placed in the same position as the invisible hand. As this was a noncorporal object, we expected it to substantially reduce the illusion (Tsakiris et al., 2010). Second, we sought to formally establish that the invisible hand illusion could be induced equally well without a rubber stump. Thus, the experiment comprised three conditions involving synchronous, spatially congruent brushing on the participant's real hand and invisible hand using a rubber stump (illusion condition), using no rubber stump (illusion condition) and using a block of wood (control condition) as depicted in Figure 3A. Similarly, a combination of questionnaires (Experiment 4a) and SCR recordings during the knife threatening of the invisible hand or block of wood (Experiment 4b) was used in two separate experiments to test the hypotheses outlined above (Figure 4).

Statistical Analysis

The Kolmogorov–Smirnoff test was used to check the normality of the data in the behavioral experiments. For normally distributed data sets, we used *t* tests to analyze differences between two conditions and repeated-measures ANOVAs to analyze differences among more than two conditions. For data sets that were not normally distributed, we used the nonparametric Wilcoxon signed-rank test to analyze differences between two conditions. Although the data were not normally distributed, we investigated the interaction effects between two main factors in a 2 × 2 factorial design and calculated the "nonparametric interaction" (referred to as "Interaction") by individually calculating the numeric difference between the two levels of each factor and then statistically comparing these differences using a Wilcoxon signed-rank test. For simplicity, two-tailed tests were used for all analyses, and the alpha was set at 5%. For experiments in which four or fewer comparisons were planned, we did not correct for multiple comparisons. When multiple planned comparisons or post hoc analyses were required we used Bonferroni-corrected alpha values.

Functional Brain Imaging Experiment

fMRI Acquisition

fMRI acquisition was performed using a Siemens TIM Trio 3T scanner equipped with a 12-channel head coil.

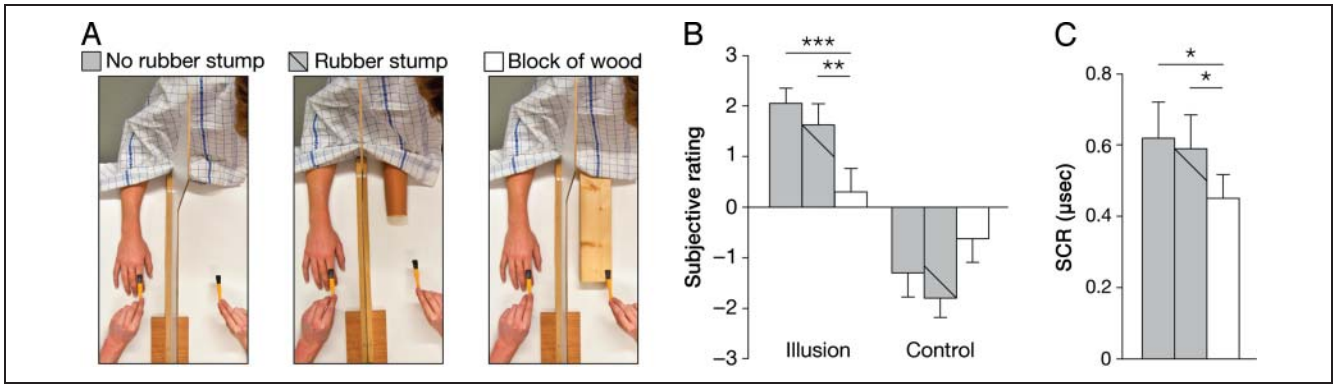

Figure 3. Experiment 4: Empty space versus noncorporeal object. (A) Experimental setup for Experiments 4a and b. (B) Experiment 4a: Average ratings of the illusion (T1–T2) and control statements (C1–C2). (C) Experiment 4b: Mean threat-evoked SCR. The error bars denote *SEM*.

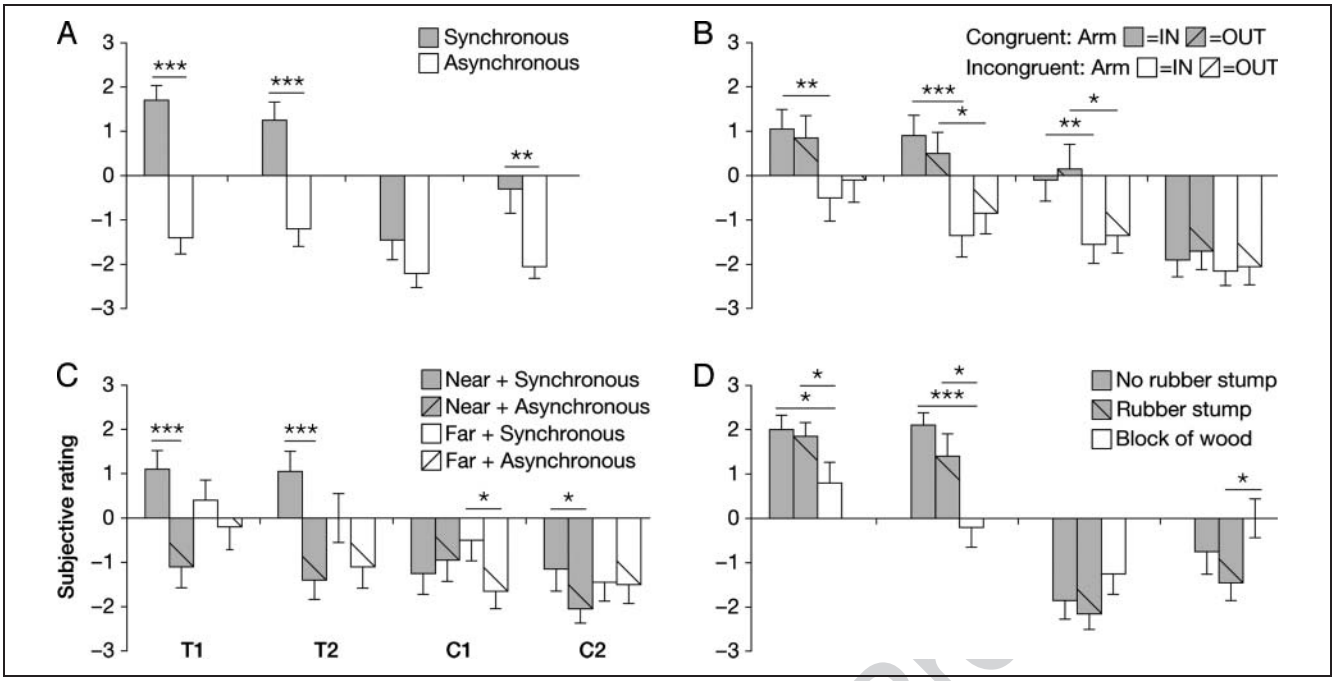

Figure 4. Mean ratings of individual questionnaire statements. Results for the questionnaire experiments: Experiment 1a (A), Experiment 2a (B), Experiment 3a (C), and Experiment 4a (D). T1–T2 = Test statements 1–2; C1–C2 = Control statements 1–2 (see Table 2). *$p < .05$, **$p < .01$, ***$p < .001$. The error bars indicate *SEM*.

Gradient-echo T2*-weighted EPIs with BOLD contrast were used as an index of brain activity (Logothetis, Pauls, Augath, Trinath, & Oeltermann, 2001). Functional image volumes were composed of 40 continuous near-axial slices with a thickness of 3 mm (with a 1-mm interslice gap), which ensured that the entire brain was within the field of view (58 × 76 matrix, 3.0 mm × 3.0 mm in-plane resolution, echo time = 40 msec). One complete volume was collected every 2.54 sec (repetition time = 2540 msec). In total, 700–800 functional volumes (depending on the illusion-onset responses of the participants) were collected for each participant and divided into three sessions. The first three volumes were discarded to account for non-steady-state magnetization. To facilitate the anatomical localization of statistically significant activations, a high-resolution structural image was acquired for each participant at the end of the experiment (3-D MPRAGE sequence, voxel size = 1 mm × 1 mm × 1 mm, field of view = 250 mm × 250 mm, 176 slices, repetition time = 1900 msec, echo time = 2.27 msec, flip angle = 9°).

Experimental Setup

During scanning, the participants laid comfortably in a supine position on the MRI bed with their head tilted ≈30° forward to permit a direct view of an MR-compatible table (42 × 35 cm with an adjustable slope) that was mounted on the bed above the subject's waist. The required head tilt was obtained by slanting the head coil using a custom-made wooden wedge with an angle of 11°. The participants' heads were additionally tilted by ≈20° within the head coil using pillows and foam pads. The participants wore MR-compatible headphones to receive the appropriate auditory stimuli. The participants' right hand was placed on the right side of the table in a fully extended posture. Care was taken to ensure that the participants could relax their hand and that the hand was placed in a comfortable position. A white cloth hid the participant's hand from view (see Figure 5A).

The experimenter used two identical paintbrushes to deliver the tactile stimulation to the participants' hidden right hand and the visual stimulation to a location that corresponded to the invisible hand, which was placed 16.5 cm to the left (as measured from the tip of the index fingers of both hands) in full view of the participants. To ensure that the magnitudes of the delivered visual and tactile stimulation were matched across the conditions (see Experimental design for details), a trained experimenter listened to audio instructions regarding the onset and nature of the forthcoming stimuli and a metronome operating at 60 beats per minute. For 12 of the 14 participants, an MR-compatible camera (MRC Systems, Heidelberg, Germany) mounted on the head coil was used to monitor eye movements. This camera recorded an image of the participant's left eye for the duration of the experiment. The video recordings were stored on a computer and analyzed off-line to confirm that the participants maintained the required fixation on the brushstrokes and to detect any undesired eye movements. We later excluded all trials in which such eye movements occurred from further fMRI analyses. All instructions to the experimenter were transmitted via a computer running Presentation 14.1

(Neurobehavioral Systems) and connected to an MR-compatible sound delivery system (NordicNeuroLab, Bergen, Norway). The same software was used to record the participants' responses and the onset times and durations of stimuli.

Experimental Design

Three experimental conditions were included in a blocked fMRI design (Ehrsson, Holmes, & Passingham, 2005). The synchronous stimulation epochs featured visuotactile stimulation that was congruent in time and space. This condition induced a vivid perceptual illusion in all of our 10 previous behavioral experiments (see Results and Figures 1–3). The incongruent stimulation epochs contained identical visual stimulation and the same degree of tactile stimulation delivered to the participant. Although they were synchronized in time, the visual and tactile stimuli were spatially incongruent in hand-centered reference frames. This condition should significantly reduce the illusion (see results of Experiment 2). The brushstrokes on the participant's real hand were delivered in a direction opposite (−180°) to that of the brushstroke stimulation of the invisible hand in full view; all other parameters were identical. The asynchronous stimulation epochs featured alternating stimulation of the invisible hand and the participant's real hand, that is, visuotactile stimulation that was spatially, but not temporally, congruent. This condition should reliably break down the illusion (see results from Experiments 1 and 3).

The duration of each individual brushstroke applied to the real or invisible hand was always 1 sec. All brushstrokes had a "long trajectory" that started at the knuckles and finished at the tip of the finger; that is, we did not apply any taps, as in Experiments 1, 3, and 4 and the pilot. The first stroke of each stimulation epoch was delivered to the little finger, and the second stroke was delivered to the ring finger. The stimulations then continued systematically to the adjacent finger from right to left and then from left to right. The frequency of the stimulations was 30 brushstrokes per minute. Consequently, during the synchronous and incongruent conditions, the visuotactile stimulation was delivered every 2 sec. In the asynchronous condition, however, the visual stimulation of the invisible hand was delayed by 1 sec relative to the tactile stimulation of the real hand. The participants were instructed to look at the tip of the brush moving in the empty space during all stimulation epochs, and their eye movements were recorded to test their compliance with this instruction (see above). This well-controlled design allowed us to hold the retinal input and tactile stimulation delivered to the digits constant across the three conditions.

During the synchronous epochs, the participants were asked to report the subjective onset of the illusion (defined as the point in time at which they began to agree with the statement "it feels as if I have an invisible hand") by

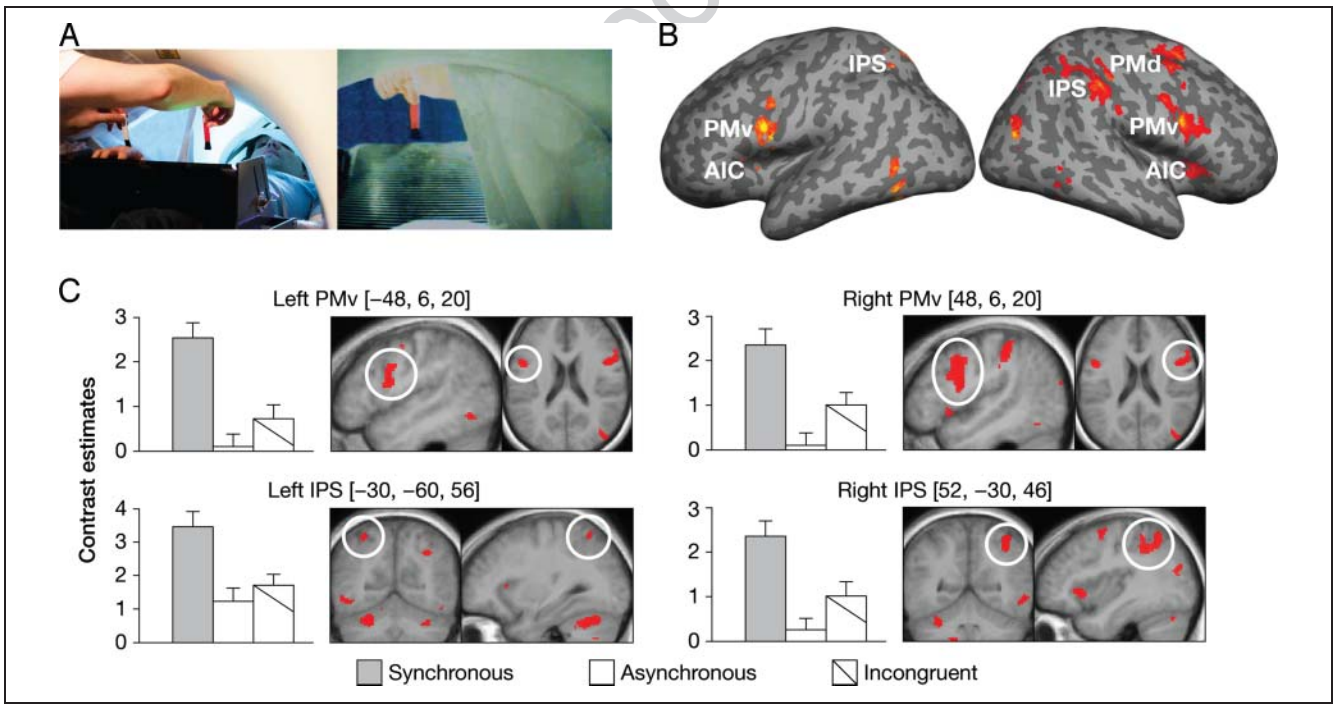

Figure 5. Experiment 5: Setup and fMRI regional analysis. (A) Experimental setup used to induce the illusion within the constrained scanner environment as observed from the outside (left) and from the participant's perspective inside the bore of the MRI scanner (right). (B, C) Significant activations that reflected the experience of having an invisible hand. All activation maps correspond to the contrast synchronous versus asynchronous ($p < .05$, FWE-corrected at the whole-brain level), which was masked inclusively with the contrast synchronous versus incongruent ($p < .001$, uncorrected). The plots display the parameter estimates for the synchronous, asynchronous, and incongruent conditions, respectively. The reported coordinates are in the MNI space. The error bars denote *SEM*. For further details, see Table 3.

pressing a button with their left hand. The onset times were recorded for each trial and used to time the presentation of tones in the headphones of the participants during the incongruent and asynchronous epochs, and the participants were instructed to respond to the tones by pressing the same button with their left hand. The visuotactile stimulation continued for a fixed period of 25 sec following the button press, which ensured that the degree of visuotactile stimulation and all motor responses were matched across conditions. A 15-sec intertrial interval separated consecutive trials. During this interval (the baseline condition), no visual or tactile stimulation occurred, and the participants were asked to fixate on a fixation point. The order of the stimulation conditions was fully randomized across sessions and participants. Each condition was repeated four times per session to yield a total of 12 trials per condition per participant. The average onset time of the illusion was 9.3 ± 5.0 sec (average ± *SD*), which agrees with previously reported onset times for the classical rubber hand illusion (Lloyd, 2007; Ehrsson et al., 2004) and is consistent with the notion that the invisible hand illusion shares the same multisensory mechanisms involved in the classical rubber hand illusion.

Postscan Behavioral Experiments

Immediately following the conclusion of brain imaging, all subjects participated in a behavioral experiment aimed at obtaining subjective and objective measurement of the illusion in a setup identical to that used during the fMRI scans. In this experiment, the participants remained in position on the MRI scanner bed with their right hand placed on the table and hidden from view as described above. We tested each condition (synchronous, asynchronous, and incongruent) once using the stimulation procedures described for the fMRI scans. To obtain subjective reports on the vividness of the illusion, participants were asked to verbally rate five statements on a scale from 0 ("*I completely disagree*") to 10 ("*I agree completely*") immediately following a period of synchronous, asynchronous, or incongruent visuotactile stimulation (adopted from Petkova et al., 2011). Statements S1–S3 were used to probe the subjective strength of the illusion, whereas S4 and S5 served as control statements (see Figure 7 for the statements). The presentation order of the experimental conditions was counterbalanced across participants.

Immediately after the questionnaire data had been collected, we registered proprioceptive drift using an intermanual pointing task as an objective index of the illusion (similar to the test used in Experiment 1c and adapted from Botvinick & Cohen, 1998). The participants were exposed to six 1-min intervals of visuotactile stimulation divided into two synchronous, two incongruent, and two asynchronous blocks. The order of these intervals was randomized. Immediately before ("premeasurement") and after ("postmeasurement") each stimulation period, participants were asked to close their eyes, and the experimenter placed the left index finger of the participants on a fixed starting position on a panel vertically aligned over the location of the real right hand and the invisible hand. Following a brief verbal cue from the experimenter, the participants were asked to swiftly move their left index finger along the panel and stop above the perceived location of the right index finger. A ruler was used to register the end position of each movement. For each trial, the difference between the pre- and postmeasurements was computed and interpreted as follows: a value > 0 represented a drift toward the location of the invisible hand; a value of 0 indicated no difference between pre- and postmeasurements; and a value < 0 corresponded to an overshoot toward the location of the real hand. The actual distance of drift was converted to a percentage of the distance between the real and invisible hands (16.5 cm). The synchronous, asynchronous, and incongruent measurements were then averaged among the participants and statistically compared at the group level (Figure 7B). Greater drift toward the invisible hand in the synchronous, as compared with the control, condition constituted our a priori-defined evidence for successful induction of the illusion.

To further corroborate the behavioral findings, we determined the correlation between the degree of proprioceptive drift and the subjectively rated strength of the illusion in the questionnaire data. Specifically, we computed an illusion index for each participant that reflected the strength of the illusion in the synchronous condition relative to the control conditions according to the equations defined below:

$$\text{synchronous versus asynchronous: } [S1 + (S2 + S3)/2 - (S4 + S5)]_{\text{SYNC}} - [S1 + (S2 + S3)/2 - (S4 + S5)]_{\text{ASYNC}}$$

$$\text{synchronous versus incongruent: } [S1 + (S2 + S3)/2 - (S4 + S5)]_{\text{SYNC}} - [S1 + (S2 + S3)/2 - (S4 + S5)]_{\text{INCONGRUENT}}$$

Subsequently, we performed a correlation analysis in which the proprioceptive drift measure was defined as the drift toward the location of the invisible hand in the synchronous condition minus the drift in this direction in the control conditions (Figure 7C).

fMRI Regional Analysis

The fMRI data from all participants were analyzed with SPM8. Following standard preprocessing (slice timing correction, realignment, coregistration, segmentation, and normalization to the Montreal Neurological Institute [MNI] standard brain), the functional images were spatially smoothed with an 8-mm FWHM isotropic Gaussian kernel. In the first analysis, we defined separate regressors for the stimulation intervals that preceded ("BEFORE BUTTON PRESS": average duration = 9.3 sec) and followed ("AFTER

BUTTON PRESS": fixed duration = 25 sec) the illusion onset, as reported by the participant with a button press or corresponding response to a tone during the control conditions. The first analysis featured the following regressors: "synchronous$_{\text{BEFORE BUTTON PRESS}}$," "synchronous$_{\text{AFTER BUTTON PRESS}}$," "asynchronous$_{\text{BEFORE BUTTON PRESS}}$," "asynchronous$_{\text{AFTER BUTTON PRESS}}$," "incongruent$_{\text{BEFORE BUTTON PRESS}}$," and "incongruent$_{\text{AFTER BUTTON PRESS}}$" for the synchronous, asynchronous and incongruent stimulation epochs. Two regressors of no interest were created to model all motor responses (button presses) and tones. Each condition was modeled with a boxcar function and convolved with the standard SPM8 hemodynamic response function. We defined linear contrasts in the general linear model (GLM; see below) to test our hypotheses. The results from this analysis are given as contrast estimates for each condition for each participant (contrast images). To accommodate intersubject variability, we entered the contrast images from all participants into a random effects group analysis (second-level analysis). To account for the problem of multiple comparisons in the statistical analysis of the whole-brain data, we report the peaks of activation that

Table 3. Areas Activated during the Illusion

Anatomical Region	*MNI x, y, z (mm)*	*Peak T*	*p*	*Cluster Size*[a]
Frontal Lobe				
L. precentral sulcus, inferior end (PMv)	−48, 6, 20	6.63	.002	257
R. precentral sulcus, inferior end (PMv)	48, 6, 20	8.16	<.001	597
L. precentral gyrus (PMd)	−50, −6, 50	5.86	.017	20
R. precentral sulcus, superior end (PMd)	52, 10, 42	7.04	.001	597
L. superior frontal sulcus	−20, 4, 52	5.82	.019	21
R. superior frontal gyrus (pre-SMA)	8, 12, 62	8.12	<.001	1125
Insular Cortex				
L. anterior insula	−32, 22, 8	6.04	.010	36
R. anterior insula	32, 24, 4	6.66	.002	245
Parietal Lobe				
L. IPS	−30, −60, 56	6.18	.007	90
R. IPS	38, −54, 54	6.72	.002	602
R. IPS, cluster extending into the supramarginal gyrus	52, −30, 46	7.45	<.001	602
Occipital Lobe				
L. lateral occipital cortex (tentative EBA)	−44, −64, −10	6.62	.002	121
R. lateral occipital cortex (tentative EBA)	56, −54, −8	6.65	.002	62
R. medial occipital gyrus	42, −80, 24	8.91	<.001	85
Subcortical Structures				
L. thalamus	−18, −26, 6	6.65	.002	49
Cerebellum				
L. cerebellum (lobe VI)	−26, −60, −28	8.17	<.001	633
L. cerebellum (lobe VIIb)	−24, −70, −44	8.17	<.001	39
R. cerebellar crus	32, −70, −28	7.10	.001	135

All brain regions (peaks) with significant activation ($p < .05$, FWE correction using the whole brain as a search space).

L = left; R = right; PMv/d = ventral/dorsal premotor cortex.

[a]Only clusters with 20 or more active voxels are listed.

achieved a significance threshold of $p < .05$ after correction using the topological family-wise error rate (FWE) implemented in SPM8. For each peak of activation, the coordinates in MNI space, t value, and p value are reported (see Table 3). In areas in which we had an a priori-defined hypothesis (premotor cortex and intraparietal cortex), we planned to use a small volume correction around the peaks from previously published studies (Ehrsson et al., 2004). However, because all of the key activations in these regions also survived the correction for multiple comparisons in the whole brain, we only used the latter, more conservative, whole-brain threshold for simplicity.

To identify the brain regions whose BOLD responses were specifically related to the invisible hand illusion, we contrasted the synchronous$_{\text{AFTER BUTTON PRESS}}$ and asynchronous$_{\text{AFTER BUTTON PRESS}}$ conditions using the statistical threshold described above (i.e., $p < .05$, corrected). This contrast is perfectly matched with respect to the magnitude of the visual and tactile stimuli and the relaxed state of the participants looking at the moving brush (i.e., no differences in task set as opposed to the "BEFORE BUTTON PRESS" period). To further control for the effect of visuotactile synchrony, we used the synchronous$_{\text{AFTER BUTTON PRESS}}$ and incongruent$_{\text{AFTER BUTTON PRESS}}$ contrast as an inclusive mask, with a significance level of $p < .001$, uncorrected. Importantly, the areas identified using this approach showed stronger activation in the illusion condition than in either of the two control conditions and thus demonstrated an activation profile that obeyed the spatial and temporal rules of the illusion as defined in our earlier behavioral experiments.

To confirm the robustness of our findings, we also swapped the order of the two comparisons in the procedure described above. Thus, we contrasted synchronous$_{\text{AFTER BUTTON PRESS}}$ and incongruent$_{\text{AFTER BUTTON PRESS}}$ ($p < .05$, corrected) and used synchronous$_{\text{AFTER BUTTON PRESS}}$ and asynchronous$_{\text{AFTER BUTTON PRESS}}$ as the inclusive mask ($p < .001$, uncorrected). All key areas representing the main findings of the experiment were also found to be significant when the data were analyzed in this manner (at $p < .05$, corrected). For simplicity, we only report the results from the first analysis in the figures and tables of this study.

For visualization purposes, an activation map featuring all significant voxels was overlaid onto a canonical inflated surface of both hemispheres using Freesurfer (Martinos Center for Biomedical Imaging, Boston, MA, USA; see Figure 5B). The contrast estimates for the synchronous$_{\text{AFTER BUTTON PRESS}}$, asynchronous$_{\text{AFTER BUTTON PRESS}}$, and incongruent$_{\text{AFTER BUTTON PRESS}}$ relative to a common baseline (the intertrial rest intervals) were extracted for all of the significant peaks of activation and are displayed as histogram plots (Figures 5 and 6). The anatomical localizations of the activations were related to the major sulci and gyri (Duvernoy, 1991) distinguishable on a mean MRI that was generated from the standardized anatomical MRIs from the 14 participants.

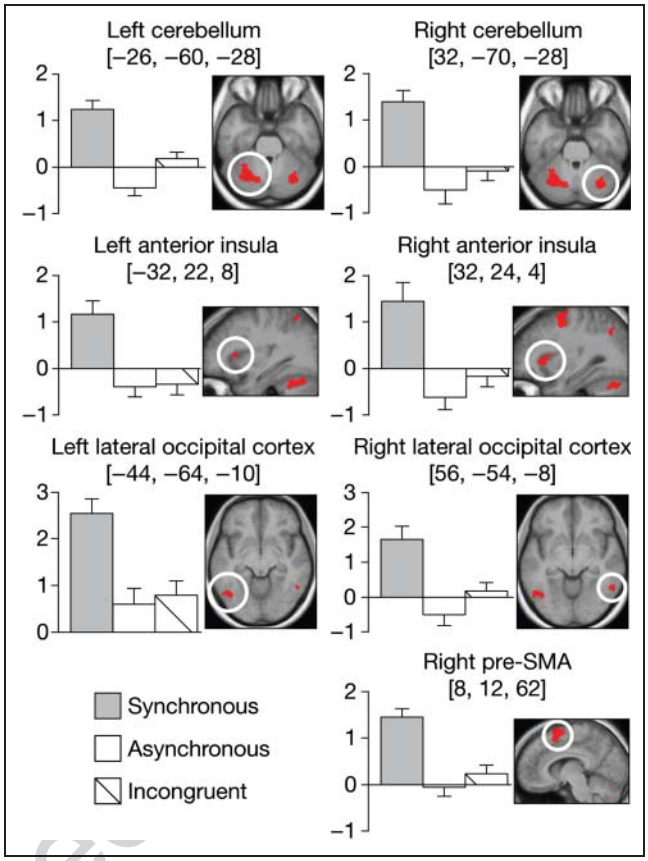

Figure 6. Activation of the cerebellum, anterior insula, lateral occipital cortex and pre-SMA. All activation maps correspond to the same contrast and statistical thresholds as in Figure 5B, C.

fMRI Connectivity Analysis

Differences in illusion-related effective connectivity were analyzed by assessing psychophysiological interactions (PPIs). The PPI indexes task- or context-induced changes in the strength of connectivity between two brain regions, as measured by a change in the magnitude of the linear regression slope that relates their underlying activities. A significant PPI indicates that the contribution of one area to another changes significantly with the experimental or psychological context (Friston et al., 1997). Connectivity changes between the left intraparietal sulcus (IPS) and the rest of the brain were assessed for condition-specific differences. We chose to place the seed in the IPS of the left hemisphere because previous studies on the rubber hand illusion consistently identified activation of the IPS contralateral to the stimulated hand (Ehrsson et al., 2004, 2005, 2007). However, because our regional GLM results revealed increased activity in the illusion condition in the bilateral IPS, we performed an identical PPI analysis using a seed region in the right IPS. In two post hoc analyses, we also placed a seed in the left cerebellum and the left lateral occipital cortex (see Discussion). The seed region was defined for each participant and consisted of the peak voxel within a 10-mm radius from the group

peak (the mean distance ± *SD* was 8.4 ± 2.2 mm) for the contrast of interest (synchronous vs. asynchronous and synchronous vs. incongruent) from which the time series (first eigenvariate) of activity was extracted. Two separate PPI analyses for each seed were performed using the contrasts synchronous versus asynchronous and synchronous versus incongruent as psychological factors. At the individual level, three regressors were created in a GLM that represented the time course of activity in the seed region (the physiological factor), the psychological factor, and their cross-product (the PPI). Contrast estimates for the PPI regressor from each participant were analyzed at the second level using one-sample *t* tests. To identify the brain regions whose activations were functionally coupled with the seed region during the illusion, the contrast estimate for the PPI regressor from the synchronous versus asynchronous PPI analysis ($p < .001$ uncorrected) was masked inclusively with the contrast estimate for the PPI regressor from the synchronous versus incongruent PPI analysis ($p < .005$ uncorrected). This inclusive masking approach allowed us to control for the potential effect of visuotactile synchrony on connectivity during the illusion. For areas for which we had a priori hypotheses, we used the significance level that corresponded to $p < .05$, FWE-corrected for multiple comparisons using a small volume correction (the relevant MNI coordinates used were derived from Gentile, Petkova, & Ehrsson, 2011). For the rest of the brain, for which we had no a priori hypotheses, we used the whole-brain topological peak FWE as implemented in SPM8.

To further corroborate our findings of neural connectivity related to the illusion, we ran two multiple regression analyses with the aim of identifying brain areas whose illusion-related increases in connectivity were significantly correlated with the participants' subjective reports and proprioceptive drift results in the postscan behavioral experiments. Specifically, we computed an illusion index from the questionnaire results for each participant (see Postscan behavioral experiments) and the difference in proprioceptive drift between the experimental conditions according to the following equation:

$$[\text{Post} - \text{measurement} - \text{Pre} - \text{measurement}]_{\text{SYNCH}} - [\text{Post} - \text{measurement} - \text{Pre} - \text{measurement}]_{\text{ASYNCH}},$$

where SYNCH and ASYNCH refer to synchronous and asynchronous conditions, respectively. We then entered the illusion indices and proprioceptive drift differences (one per participant) as covariates in two separate, second-level multiple regression analyses and evaluated significant ($p < .001$ uncorrected) positive correlations with the PPI contrast estimates (from the synchronous versus asynchronous PPI analysis) in a whole-brain voxel-wise fashion. Because these correlation analyses test for variability related to interindividual differences in illusion ratings or proprioceptive drift measures in addition to the main effect of the PPI term, we did not need to control for visuotactile synchrony in this analysis. It is important to note that these correlation analyses are independent, hence not circular, from the analysis that led to the identification of voxels displaying significant illusion-related connectivity.

RESULTS

Experiment 1: Temporal Congruency

The first aim was to test the prediction that the illusion would depend on temporally correlated visual and tactile signals. In Experiment 1a–c, we compared synchronous or asynchronous visual and tactile brushstrokes applied to the real and invisible hands (Figure 1A). Our results showed that, compared with the asynchronous condition, participants in the synchronous condition affirmed the statements in the questionnaires that reflected the illusory percept more strongly than they affirmed the control statements (for the ratings of each individual statement, see Figure 4) (Figure 1B: interaction Statement Type × Condition: $Z = -3.283$, $p = .001$; Experiment 1a), displayed a greater threat-evoked SCR when the invisible hand was stabbed with a knife (Figure 1C: $t = 3.541$, $p = .001$; Experiment 1b) and demonstrated greater proprioceptive drift toward the location of the invisible hand (Figure 1D: $t = 3.005$, $p = .007$; Experiment 1c). Thus, the elicitation of the invisible hand illusion depends on a temporally correlated visuotactile stimulation.

Experiments 2 and 3: Spatial Congruency and Reference Frame

The subsequent experiments probed the spatial constraints of the illusion. We hypothesized that the visual and tactile touches necessary to evoke the illusion must be spatially congruent in relation to a hand-centered reference frame defined by the proprioceptive signals from the real arm (Costantini & Haggard, 2007) and restricted to the space near the body (Lloyd, 2007). To test this hypothesis, we first implemented a 2 × 2 factorial design in which we independently manipulated the posture of the real arm and direction of the visually presented brushstrokes (Experiment 2a–b). There were two different arm positions (90° angular difference) and two different stroking directions (also a 90° angular difference) that were congruent or incongruent in the hand-centered coordinates (Figure 2A). The congruent condition induced significantly more affirmative ratings of the illusion statements than the control statements (Figure 2B: interaction Statement Type × Condition: $Z = -2.109$, $p = .035$; Experiment 2a) and a greater threat-evoked SCR (Figure 2C: $t = 2.977$, $p = .006$; Experiment 2b) compared with the incongruent control condition. Thus, the spatial congruency necessary to elicit the illusion is defined in a hand-centered frame of reference.

We further predicted that the illusion would only work when congruent multisensory stimuli were presented in the space near the body because the receptive fields of neurons encoding visual stimuli in hand-centered coordinates are restricted to peripersonal space (Brozzoli et al., 2011; Làdavas & Farnè, 2004). Therefore, we employed a 2 × 2 factorial design (distance and timing) in which the visual stimulation in the empty space was within the participant's reaching space ("near") or in the extrapersonal space outside the limits of the participants' reach ("far") during synchronous or asynchronous visuotactile stimulation (Experiment 3a–b; Figure 2D). The illusion condition near + synchronous generated higher ratings for the illusion statements than for the control statements (Figure 2E: interaction Statement Type × Distance × Timing: $F(1, 39) = 13.768$, $p = .001$; Experiment 3a) and greater threat-evoked SCRs (Figure 2F: interaction Distance × Timing: $F(1, 21) = 5.403$, $p = .030$; Experiment 3b) than the three control conditions. Thus, the multisensory mechanisms involved in the invisible hand illusion operate exclusively in the space near the body.

Experiment 4: Empty Space versus a Noncorporeal Object

Previous studies have shown that body ownership illusions cannot be induced with objects that do not visually resemble a human body part. If this is true, then why is the invisible hand illusion possible? We hypothesized that the illusion is elicited because the congruent visuotactile stimuli are presented in empty space where there is no physical object present that provides unambiguous visual evidence against the referral of somatic sensations to this location. Therefore, in Experiment 4a–b, we directly compared the synchronous invisible hand condition with a condition in which a block of wood was presented in the same position as the invisible hand (Figure 3A). Our results show that in the two invisible hand illusion conditions ("rubber stump" and "no rubber stump"[1]) compared with visual stimulation applied to the block of wood ("wood" control condition), the participants more strongly affirmed the illusion statements (Figure 3B: $Z = -3.581$, $p < .001$ and $Z = -3.557$, $p < .001$, respectively; Experiment 4a) and showed greater threat-evoked SCRs (Figure 3C: $F(2, 58) = 4.534$, $p = .042$; planned comparisons *stump* vs. *wood*: $t = 2.129$, $p = .042$; *no stump* vs. *wood*: $t = 2.539$, $p = .017$; Experiment 3b). Thus, the presence of a noncorporeal object appears to suppress the perceptual binding of visual and tactile signals, thereby preventing the referral of somatic sensations to the same portion of space.

Experiment 5: Neural Mechanisms

The behavioral experiments reported above (Experiments 1–4) identified the perceptual rules of the invisible hand illusion and suggest that multisensory integration in a hand-centered reference frame is the underlying neural mechanism. We therefore predicted that fMRI would reveal increased neuronal activity in key multisensory areas in the premotor and intraparietal cortices during periods when the participants experienced the illusion (see Introduction and Discussion for details; Brozzoli et al., 2012; Ehrsson et al., 2004). As described in the Methods section, we developed a setup in which we could reliably induce the invisible hand illusion in the constrained environment of an MRI scanner (Figure 5A) and measured the BOLD signals in 14 participants who experienced a vivid illusion (see Figure 7A–C for confirmatory postscan behavioral results). To identify the areas that were specifically associated with this perceptual experience, we compared the illusion condition, which consisted of synchronous and isodirectional brushstrokes applied to the hidden real hand and the invisible hand (synchronous), with two control conditions in which asynchronous isodirectional brushstrokes (asynchronous) or synchronous and opposing brushstrokes were employed (incongruent). This design strategy allowed us to maintain identical retinal input and match the amount of tactile stimulation across all three conditions while controlling for the effect of visuotactile synchrony.

fMRI Regional Analysis

In support of our hypothesis, we observed significant activations in the bilateral ventral premotor cortices (Figure 5B, C: left PMv: $t = 6.63$, $p = .002$, right PMv: $t = 8.16$, $p < .001$) (all reported coordinates are in the MNI space, and the p values have been corrected for multiple comparisons at the whole-brain level) and bilateral IPS (Figure 5B, C: left IPS: $t = 6.18$, $p = .007$, right IPS: $t = 7.45$, $p < .001$). In addition, we found significant activations in two other structures related to the processing of sensory signals from the body, namely the bilateral anterior insular cortices (Figure 6: left AIC: $t = 6.04$, $p = .010$, right AIC: $t = 6.66$, $p = .002$) and cerebellum (Figure 6: left: $t = 8.17$, $p < .001$, right: $t = 7.10$, $p < .001$). We also found significant activation in the bilateral lateral occipital cortices and in the right pre-SMA (see Table 3 and Figure 6). Whereas the pre-SMA is the target of dense anatomical connections from the pFC and is important for internally generated actions (Passingham, Bengtsson, & Lau, 2010), it receives relatively little input from sensory association areas in the parietal cortex (Passingham, 1993). It is therefore an unlikely candidate for the implementation of basic multisensory integrative mechanisms mediating the construction and maintenance of a cortical representation of the body. Thus, the discussion will focus primarily on the multisensory frontoparietal circuits for which we had strong a priori hypotheses. In summary, our imaging data strongly associate the perceptual processes of the invisible hand illusion with regional activity in multisensory areas related

to the integration of visual and tactile signals in hand-centered reference frames.

fMRI Connectivity Analysis

Given the established view that the premotor and posterior parietal cortices work as nodes of a densely interconnected neural circuit (Rizzolatti, Luppino, & Matelli, 1998) and the coactivation of these regions in this study, we decided to investigate changes in connectivity between the areas that were specific to the illusion. We hypothesized that the activation of the IPS and PMv reflected the response properties of multisensory neuronal populations working in concert to represent the invisible hand; therefore, an increased functional coupling between these two areas should be observable during the illusion. To examine this prediction, a whole-brain PPI analysis was performed using a seed region in the left IPS. In support of our hypothesis, we found that the experience of the illusion increased the functional coupling to the left ventral premotor cortex (Figure 8A, B: $t = 5.32$; $p = .012$ after small-volume correction), the most anterior section of the IPS at the junction with the postcentral sulcus (Figure 8C: $t = 5.67$; $p = .008$, after small-volume correction) and the supramarginal gyrus (Figure 8D: $t = 4.08$; $p = .059$, after small-volume correction).

Importantly, the illusion-induced increases in connectivity with the left PMv were positively correlated with questionnaire illusion ratings (Figure 8E: $t = 5.60$; $p = .019$, after small-volume correction) and the proprioceptive drift (Figure 8F: $t = 4.27$; $p = .065$, after small-volume correction) measured in the postscan behavioral experiments, which demonstrates a systematic relationship between the strength of the illusion and the strength of effective connectivity between the intraparietal and premotor cortices.

To test for interhemispheric connectivity changes, we performed a separate analysis using a seed region in the right IPS. The illusion experience increased the functional coupling between the right IPS and the contralateral left premotor cortex (−50, 0, 36; $t = 5.66$; $p = .008$, after

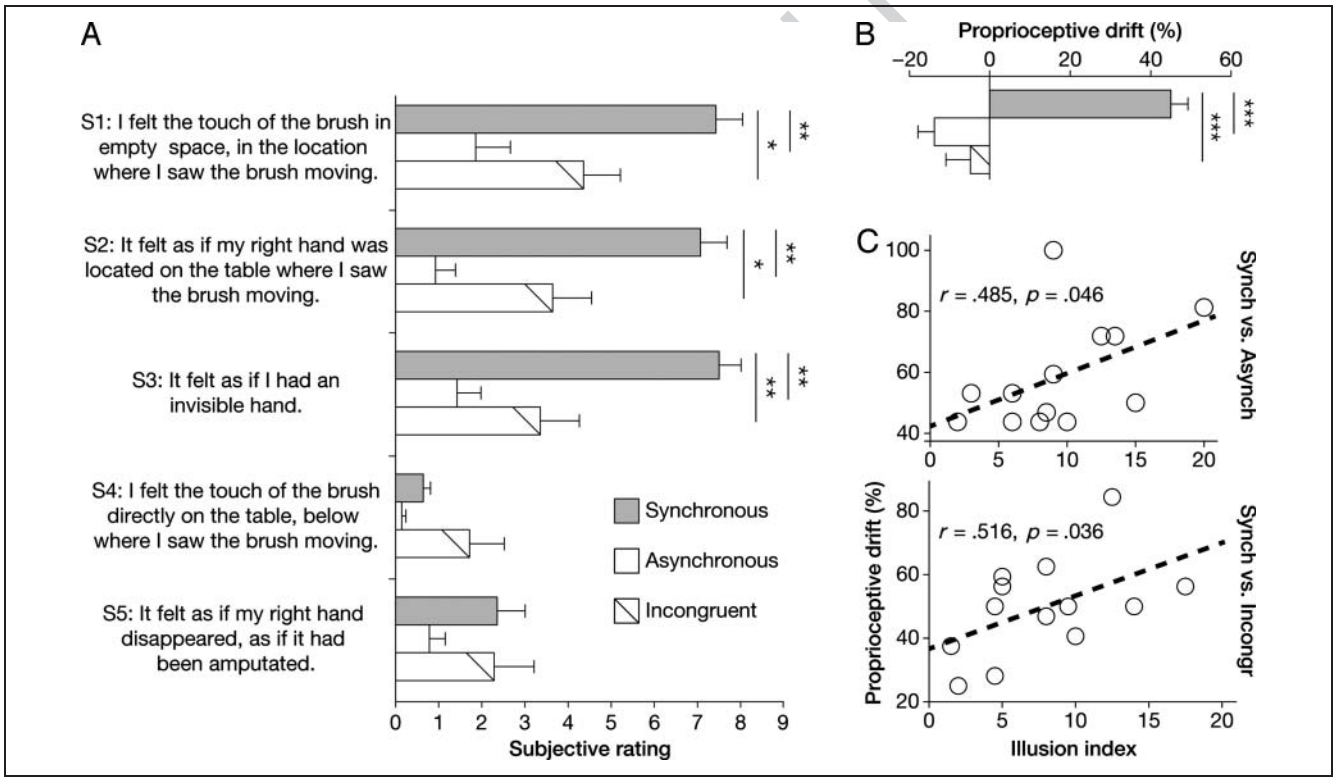

Figure 7. Postscan behavioral results. (A) The results from the postscan questionnaire. The participants rated the illusion statements (S1–S3) significantly higher in the synchronous condition than in the asynchronous and incongruent conditions. However, no such difference was observed for the control statements (S4–S5). (B) The postscan proprioceptive drift results demonstrate that, in the synchronous condition, the participants had significantly greater drift toward the location of the invisible hand than in the asynchronous and incongruent conditions. The drift is expressed as the percentage of the total distance between the real and invisible hands (16.5 cm), and positive values indicate a drift in the direction toward the invisible hand. (C, D) The difference in drift was correlated with the difference in the subjective illusion strength when comparing the synchronous and asynchronous conditions and synchronous and incongruent conditions. These results are thus consistent with the behavioral data from Experiment 1c and demonstrate that the proprioceptive drift is greater in the illusion condition than the control condition with spatially incongruent synchronous stimulation. In addition, these results confirm the expected correlation between the subjective illusion strength and proprioceptive drift magnitude based on rubber hand illusion experiments (Costantini & Haggard, 2007; Tsakiris et al., 2006; Tsakiris & Haggard, 2005; Botvinick & Cohen, 1998). The error bars denote the *SEM*. $*p < .05$, $**p < .01$, $***p < .001$.

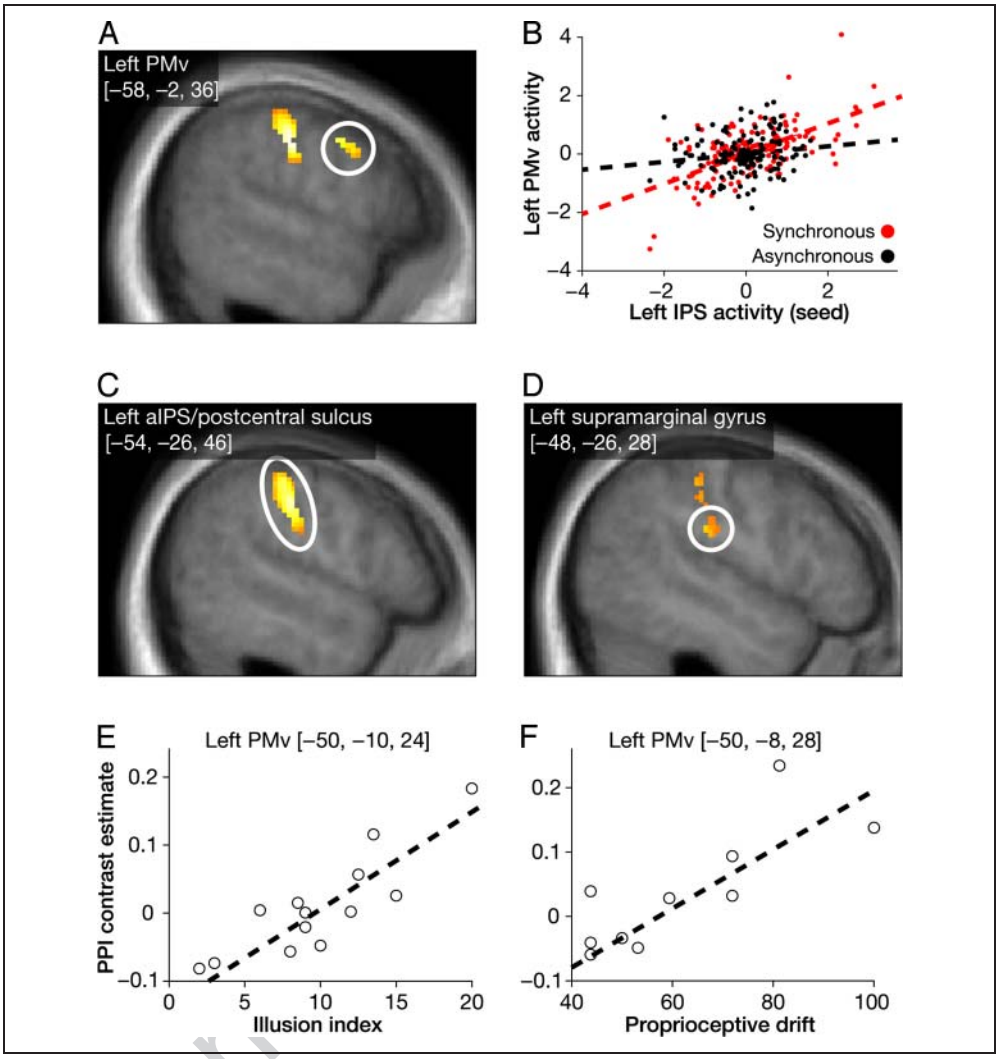

Figure 8. fMRI connectivity analysis. (A–D) Illusion-related increases in connectivity to the seed region in the left IPS were found in the left PMv and parietal regions (threshold at $p < .005$, uncorrected for display purposes). B displays the result of the PPI analysis for the PMv peak from a representative subject. Measurements during the synchronous illusion condition are indicated by red circles, whereas measurements during the asynchronous control condition are indicated by black circles. The regression slopes of the respective conditions are indicated by red and black lines. Corrected activity (in arbitrary units) in the left PMv is displayed as a function of the corrected activity in the left IPS (the seed region). (E–F) The degree of connectivity increase between the IPS seed and left PMv during the illusion (PPI contrast estimate, with synchronous versus asynchronous as the psychological factor) was correlated with the subjective illusion strength (Illusion index for synchronous vs. asynchronous) and the degree of pointing error toward the invisible hand (proprioceptive drift difference between synchronous and asynchronous) in the postscan behavioral experiments.

small-volume correction) and supramarginal gyrus (−48, −24, 26; $t = 4.97$; $p = .018$, after small-volume correction). In contrast to the ipsilateral seed region, we observed no significant correlations with the postscan questionnaire and proprioceptive drift results.

In a post hoc analysis, we also probed for possible illusion-related changes in effective connectivity in two other circuits, namely, between the cerebellum and frontoparietal cortex and between the posterior parietal cortex and the lateral occipital cortex (tentative "extrastriate body area" [EBA]). When the left lateral cerebellum served as the seed region, we observed illusion-related increases in connectivity with the ipsilateral premotor cortex (−58, −2, 34; $t = 7.32$; $p < .001$ uncorrected), and with the anterior (−56, 28, 46; $t = 7.33$; $p < .001$ uncorrected) and medial (−34, −36, 46; $t = 5.62$; $p < .001$ uncorrected) portions of the IPS. When the left lateral occipital cortex was selected as seed region, we found illusion-induced increases in connectivity with the dorsal premotor cortex (−36, −2, 62; $t = 6.29$; $p < .001$ uncorrrected) and the IPS (−44, −32, 40; $t = 5.03$; $p < .001$ uncorrected). None of these PPIs were significantly correlated with questionnaire illusion ratings or proprioceptive drift results.

DISCUSSION

This study reports a perceptual illusion in which healthy participants experience a referral of somatic and ownership sensations to a discrete volume of empty space that was fully visible to them, thereby evoking the experience of having an invisible hand. This effect was supported by complementary questionnaire, behavioral, psychophysiological, and fMRI evidence from 11 independent experiments. Two main conclusions can be drawn from the data. First, the behavioral experiments showed that the illusion depends on temporal synchrony and spatial congruency, with respect to hand-centered reference

frames and within near-personal space, of the visual and tactile stimuli. Second, the fMRI experiment showed that the illusion is associated with activations in areas related to the multisensory integration of body signals, most notably the ventral premotor and the intraparietal cortices, and with enhanced effective connectivity between these two regions. These findings challenge the assumption that when vision is used, visual information from the body itself plays a crucial role in bodily self-perception. The results also have implications for models of body ownership and provide insight regarding the underlying frontoparietal mechanisms.

The Role of Vision in Bodily Self-attribution

The invisible hand illusion challenges the view that only a physical object that visually resembles a humanoid body part can elicit an illusory feeling of ownership (Petkova et al., 2011; Tsakiris et al., 2010; Petkova & Ehrsson, 2008; Tsakiris & Haggard, 2005). This phenomenon is different from the localization of limbs in the absence of vision, for example, when the hand is occluded or in the dark. In these situations, the brain must rely on other sensory modalities to maintain an accurate representation of the hand location, but no illusory change in self-attribution is elicited. The invisible hand illusion also differs from the "somatic rubber hand illusion," in which blindfolded individuals experience touching their own hand when they are in fact touching a rubber hand (Ehrsson et al., 2005). Whereas the somatic rubber hand illusion is solely based on tactile-proprioceptive integration, the invisible hand illusion shows that visual information that provides clear evidence that a hand is not present at a specific location can be overridden by specific spatiotemporal patterns of visuotactile signals. However, the presence of a physical object that did not resemble a limb eliminated the illusion (Experiment 4). These results suggest that the visual signals contributing to the multisensory integration processes underlying illusory changes in limb self-attribution must be centered upon a human-like hand (as in the case of the rubber hand illusion) or unexpectedly, an empty volume of space, but not a noncorporeal object. This conclusion begs the question: Why can empty space be embodied as one's own hand but not noncorporeal objects? We propose that the crucial difference lies in that we are very used to feeling our hands without seeing them, and we can move our hands in empty space but not through solid objects. Unlike the space occupied by noncorporeal objects, the empty space close to the body represents an array of potential locations for the limbs. This specific property of the peripersonal empty space does not prevent visuotactile integrative mechanisms from updating the spatial location of the hand to a new anatomically plausible location in empty space. In summary, the invisible hand illusion shows that visual information from a body part itself is not a necessary factor for visuotactile-proprioceptive integration mechanisms to induce changes in the spatial boundaries of the perceived bodily self.

Models of the Rubber Hand Illusion and Body Ownership

Our results suggest that the invisible hand illusion depends on the same neural mechanisms as the classical rubber hand illusion. Both perceptual phenomena appear to obey the same multisensory spatiotemporal principles and share analogous neural substrates in the premotor and intraparietal cortices. Thus, the invisible hand illusion has relevant implications for existing models of the classical rubber hand illusion. These models have proposed that a match between (i) the visual appearance of the viewed object and implicit knowledge of the shape of human body parts (Tsakiris, 2010) and (ii) the visually perceived orientation of the rubber hand and the felt posture of the hidden real hand (visuoproprioceptive match) (Blanke, 2012; Ehrsson, 2012; Moseley et al., 2012; Makin et al., 2008) are essential prerequisites for inducing the illusion. The invisible hand illusion, however, clearly demonstrates that (i) and (ii) are not necessary conditions for illusory changes in hand ownership to occur because such changes could be induced in the absence of visual information from a rubber hand. Thus, it appears that the neural mechanisms underlying the classical rubber hand illusion are surprisingly not dependent upon the visual presence of a rubber hand. From the broader perspective of models of bodily self-perception (Blanke, 2012; Ehrsson, 2012; Moseley et al., 2012; Tsakiris, 2010; Makin et al., 2008), the current data support the view that illusory changes in the feeling of body ownership can be generated by correlated signals in different combinations of sensory modalities (Kalckert & Ehrsson, 2012; Walsh, Moseley, Taylor, & Gandevia, 2011; Tsakiris, Prabhu, & Haggard, 2006; Ehrsson et al., 2005). For example, one study reported that the rubber hand illusion can be elicited by matching visual and proprioceptive signals when tactile signals are blocked by digital anesthesia (Walsh et al., 2011). In line with the present results, what appears to be important for changes in body ownership is that the specific spatiotemporal pattern of signals in at least two sensory modalities obeys basic multisensory integration principles and provide meaningful information about the location and self-identity of the limb.

In contrast, Ramachandran and colleagues have proposed a model of the rubber hand illusion in which the feeling of ownership of the fake hand is the consequence of Bayesian perceptual learning based solely on the detection of temporally correlated visual and tactile signals (Armel & Ramachandran, 2003). This model predicts that the illusion should be elicited for objects that do not resemble human body parts (e.g., a tabletop) and objects that are presented far from the body. However,

several studies have failed to replicate an ownership illusion for noncorporeal objects (Petkova et al., 2011; Tsakiris et al., 2010; Haans et al., 2008; Petkova & Ehrsson, 2008; IJsselsteijn et al., 2006; Tsakiris & Haggard, 2005) or rubber hands placed in extrapersonal space (Lloyd, 2007). Moreover, the data in Armel and Ramachandran's original study appear to be incompatible with this model because the amplitude of both the subjective and physiological responses was significantly lower in the "table illusion" condition compared with the rubber hand illusion (Armel & Ramachandran, 2003). One study reported that inducing a version of the rubber hand illusion using virtual reality technology and then instantaneously replacing the owned virtual hand with a neutral white box can cause the referral of touch onto the box (Hohwy & Paton, 2010). This study, however, did not measure the extent to which the participants perceived the box to be part of their own body, and the illusory referral of touch could only be induced after a period of prior exposure to the rubber hand illusion. The present results are incompatible with the model proposed by Ramachandran and colleagues for three reasons. First, the invisible hand illusion could not be elicited by visuotactile stimulation that was temporally synchronous but spatially incongruent (Experiment 2). Second, the experience of the illusion could not be triggered when the visual stimulation originated outside of near-personal space (Experiment 3). Finally, the block-of-wood condition in Experiment 4 did not elicit an illusion, which directly contradicts the notion that temporally correlated visuotactile signals can induce ownership sensations for noncorporeal objects.

Premotor–Intraparietal Circuits

We found that the experience of the illusion was associated with increases in the BOLD response and stronger effective connectivity between the premotor and intraparietal cortices. These regions are ideal candidates for mediating the multisensory integrative processes that underlie the invisible hand illusion. Neurophysiological studies in nonhuman primates have demonstrated that these areas contain neuronal populations that have the capacity to integrate visual, tactile, and proprioceptive signals and support a central representation of the hand in space (Graziano, 1999, 2000; Graziano et al., 1997a; Rizzolatti, Scandolara, Matelli, & Gentilucci, 1981). In humans, previous fMRI studies have shown that these areas contain neuronal populations that respond preferentially to visual stimuli in near-personal space (Brozzoli et al., 2011, 2012; Makin, Holmes, & Zohary, 2007). Furthermore, their activity is increased when individuals observe their own real hand being touched (Gentile et al., 2011; Lloyd, Shore, Spence, & Calvert, 2003) and during periods when participants experience the classical rubber hand illusion (Brozzoli et al., 2012; Ehrsson et al., 2004, 2007). In the present illusion, the referral of somatic and ownership sensations to empty space is likely associated with a shift in a hand-centered spatial reference frame from the hidden real hand toward the location of the invisible hand, which is in line with the notion that shifts in hand-centered visual receptive fields appear to occur during the rubber hand illusion (Brozzoli et al., 2012; Graziano, 2000). The finding that illusion-related premotor and intraparietal activation is independent of visual feedback from a rubber hand is consistent with fMRI data from the somatic rubber hand illusion in blindfolded participants (Ehrsson et al., 2005) and the observation that cells in the premotor and intraparietal cortices encode the location of the arm even when it is not directly visible to the monkey (Obayashi, Tanaka, & Iriki, 2000; Graziano, 1999) or is in the dark (Graziano, Hu, & Gross, 1997b). Thus, the premotor-intraparietal activity measured here are interpreted to reflect the multisensory integrative processes that are related to the recalibration of a central representation of one's own body to incorporate an external hand— visible or invisible—into this representation.

In our incongruent control condition, we selectively manipulated the directionality of the tactile stimuli while holding the visual input constant and showed that both the subjective illusion experience and associated activity in premotor and intraparietal areas decreased. Our results therefore extend previous fMRI studies on the rubber hand illusion by demonstrating that the activation of these areas is contingent upon the spatial congruence between the seen and felt touches, which is an important prediction of multisensory models of limb ownership (Ehrsson, 2012; Makin et al., 2008) and multisensory integration theory (Stein & Stanford, 2008; Avillac, Denève, Olivier, Pouget, & Duhamel, 2005; Holmes & Spence, 2005).

Finally, our study is the first to report enhanced effective connectivity between the ventral premotor and intraparietal cortices in the context of body ownership illusions. Crucially, this increase was positively correlated with the subjective strength of the illusion and the proprioceptive drift. These results strengthen the notion that distributed neural processing in interconnected premotor-intraparietal circuits (Graziano & Cooke, 2006; Marconi et al., 2001; Rizzolatti et al., 1998) reflects the updating of the spatial boundaries of the body and the associated feeling of limb ownership. Moreover, this finding corroborates the idea that the activity in the ventral premotor cortex observed during previously published body ownership illusions (Brozzoli et al., 2012; Petkova et al., 2011; Ehrsson et al., 2004, 2005) is likely to depend on input from the intraparietal cortex.

Activations in Cerebellar, Insular, and Lateral Occipital Regions

We also observed activations in the cerebellar, insular and lateral occipital regions that are worth discussing. The cerebellar activation was located in a section of the lateral cerebellum that is anatomically connected to the posterior parietal and premotor cortices (Clower, West, Lynch, &

Strick, 2001; Orioli & Strick, 1989). This section of the cerebellum has the capacity to integrate body-related visual, tactile, and proprioceptive signals (Dum, Li, & Strick, 2002) and has been reported to be active in rubber hand illusion studies (Ehrsson et al., 2004, 2005) and during the delivery of synchronized visuotactile stimulation on a person's real hand (Gentile et al., 2011). This region is considered to compute the temporal relationship between sensory and motor signals (Ito, 2000; Miall, Weir, Wolpert, & Stein, 1993) and is involved in the generation of sensory predictions (Blakemore, Frith, & Wolpert, 2001). We propose that the cerebellar activation observed here reflects the neuronal computations that are needed to generate precise predictions of expected tactile signals based on the visual impressions from the paintbrush moving in empty space. This information is then made available to frontoparietal circuits that construct a representation of the body in space. This notion is supported by the observed increase in connectivity between the cerebellum and premotor and intraparietal cortices during the illusion.

Notably, we observed activation in the lateral occipital cortex at a location in stereotactic space that was consistent with the EBA (Figure 6). This area is a subregion of the occipital lobe that is selectively activated by the visual perception of bodies (Downing & Peelen, 2011; Downing, Jiang, Shuman, & Kanwisher, 2001) and considered to play an important role in the perceptually relevant processing of body parts (Downing & Peelen, 2011; Myers & Sowden, 2008). Given that the participants did not directly observe a body part at the location of their perceived hand and that the visual input was matched between our experimental conditions, this result suggests that merely viewing a part of space that is represented as "self" appears to activate the EBA. We propose that multisensory integrative mechanisms in frontoparietal areas constructing a representation of the body in space modulate the activity in this body-sensitive high-level visual area, which is in line with our post hoc observation of increased functional coupling with the intraparietal cortex during the illusion. This view is compatible with evidence suggesting that tactile, proprioceptive, and motor signals from the upper limb modulate the response in lateral occipital regions devoted to the processing of visual information from the same body part (Costantini, Urgesi, Galati, Romani, & Aglioti, 2011; Orlov, Makin, & Zohary, 2010; Astafiev, Stanley, Shulman, & Corbetta, 2004). Further experiments are needed to corroborate this interpretation.

We also observed illusion-related activity in the anterior insular cortex, which suggests that the illusion induces changes in the interoceptive system (Craig, 2002). The anterior insula is strongly connected with higher sensory areas (Mesulam & Mufson, 1982); however, it has not been directly implicated in the basic multisensory integration mechanisms that are associated with the rubber hand illusion (Ehrsson et al., 2004, 2005, 2007). The present activation should not be mistaken for the posterior insula cluster that was reported to correlate with the proprioceptive drift in a study conducted by Tsakiris and colleagues (Tsakiris, Hesse, Boy, Haggard, & Fink, 2007). We speculate that the anterior insular activity reflects changes in the interoceptive system that are coupled with the emotional responses triggered by the invisible hand illusion.

Physical and Nonphysical Body Parts

The invisible hand illusion challenges the implicit assumption that healthy nonamputated individuals can only experience physical objects as part of their own body. To the best of our knowledge, the explicit experience of embodying a "nonphysical" limb in the present illusion differs from all of the previously reported body illusions, including the rubber hand illusion (Botvinick & Cohen, 1998), full-body illusions (Guterstam & Ehrsson, 2012; Petkova & Ehrsson, 2008; Ehrsson, 2007; Lenggenhager et al., 2007), illusory "telescoping" of the hand (Schmalzl & Ehrsson, 2011), and the cutaneous rabbit illusion, in which the rabbit "hops out of the body" (Miyazaki, Hirashima, & Nozaki, 2010). The experience of an invisible hand is also different from the projection of tactile sensations to the tip of hand-held tools (Maravita & Iriki, 2004) or illusory feelings of bodily movement evoked by visuoproprioceptive integration in hand-laterality judgments (Viswanathan, Fritz, & Grafton, 2012), in which the sense of hand ownership appears to be unchanged. The only perceptual phenomena that appear to share the key feature of attributing an invisible limb to the bodily self are phantom limbs, which are often reported by amputees (Flor, Nikolajsen, & Jensen, 2006; Ramachandran & Hirstein, 1998). Future studies should examine the potential similarities between phantom limbs and the invisible hand illusion in terms of multisensory processes and neural mechanisms.

Acknowledgments

This study was funded by the European Research Council, the Swedish Foundation for Strategic Research, the Human Frontier Science Program, the McDonnell Foundation, and Söderbergska Stiftelsen. A. G. and G. G. are registered Ph.D. students in the Stockholm Brain Institute graduate program. We also thank Laura Schmalzl for valuable discussions. The fMRI scans were conducted at the MR Centre at the Karolinska University Hospital Huddinge.

Reprint requests should be sent to Arvid Guterstam, Retzius väg 8, SE-17177 Stockholm, Sweden, or via e-mail: arvid.guterstam@ki.se.

Note

1. Minor note: In Experiment 4, we included two versions of the invisible hand illusion (Figure 3A), one with a rubber stump present just below the invisible hand (as used in the Pilot and Experiment 1, see Figure 1) and one without the rubber stump (Experiments 2 and 3). The illusion worked equally well in both conditions; there were no significant differences in terms of subjective ratings or threat-evoked SCR between the "*rubber stump*" and "*no rubber stump*" conditions (see Figure 3B-C).

REFERENCES

Armel, K. C., & Ramachandran, V. S. (2003). Projecting sensations to external objects: Evidence from skin conductance response. *Proceedings of the Royal Society of London, Series B, Biological Sciences, 270,* 1499–1506.

Astafiev, S. V., Stanley, C. M., Shulman, G. L., & Corbetta, M. (2004). Extrastriate body area in human occipital cortex responds to the performance of motor actions. *Nature Neuroscience, 7,* 542–548.

Avillac, M., Denève, S., Olivier, E., Pouget, A., & Duhamel, J.-R. (2005). Reference frames for representing visual and tactile locations in parietal cortex. *Nature Neuroscience, 8,* 941–949.

Bahrick, L. E., & Watson, J. S. (1985). Detection of intermodal proprioceptive–visual contingency as a potential basis of self-perception in infancy. *Developmental Psychology, 21,* 963–973.

Blakemore, S. J., Frith, C. D., & Wolpert, D. M. (2001). The cerebellum is involved in predicting the sensory consequences of action. *NeuroReport, 12,* 1879–1884.

Blanke, O. (2012). Multisensory brain mechanisms of bodily self-consciousness. *Nature Reviews Neuroscience, 13,* 556–571.

Botvinick, M., & Cohen, J. (1998). Rubber hands "feel" touch that eyes see. *Nature, 391,* 756.

Brozzoli, C., Gentile, G., & Ehrsson, H. H. (2012). That's near my hand! Parietal and premotor coding of hand-centered space contributes to localization and self-attribution of the hand. *The Journal of Neuroscience, 32,* 14573–14582.

Brozzoli, C., Gentile, G., Petkova, V. I., & Ehrsson, H. H. (2011). fMRI adaptation reveals a cortical mechanism for the coding of space near the hand. *The Journal of Neuroscience, 31,* 9023–9031.

Clower, D. M., Hoffman, J. M., Votaw, J. R., Faber, T. L., Woods, R. P., & Alexander, G. E. (1996). Role of posterior parietal cortex in the recalibration of visually guided reaching. *Nature, 383,* 618–621.

Clower, D. M., West, R. A., Lynch, J. C., & Strick, P. L. (2001). The inferior parietal lobule is the target of output from the superior colliculus, hippocampus, and cerebellum. *The Journal of Neuroscience: The Official Journal of the Society for Neuroscience, 21,* 6283–6291.

Costantini, M., & Haggard, P. (2007). The rubber hand illusion: Sensitivity and reference frame for body ownership. *Consciousness and Cognition, 16,* 229–240.

Costantini, M., Urgesi, C., Galati, G., Romani, G. L., & Aglioti, S. M. (2011). Haptic perception and body representation in lateral and medial occipito-temporal cortices. *Neuropsychologia, 49,* 821–829.

Craig, A. D. (2002). How do you feel? Interoception: The sense of the physiological condition of the body. *Nature Reviews Neuroscience, 3,* 655–666.

Dawson, M., Schell, A., & Filion, D. (2007). The electrodermal system. In J. Cacioppo, L. Tassinary, & G. Berntson (Eds.), *The handbook of psychophysiology* (pp. 152–191). Cambridge: Cambridge University Press.

Downing, P. E., Jiang, Y., Shuman, M., & Kanwisher, N. (2001). A cortical area selective for visual processing of the human body. *Science (New York, N.Y.), 293,* 2470–2473.

Downing, P. E., & Peelen, M. V. (2011). The role of occipitotemporal body-selective regions in person perception. *Cognitive Neuroscience, 2,* 186–203.

Dum, R. P., Li, C., & Strick, P. L. (2002). Motor and nonmotor domains in the monkey dentate. *Annals of the New York Academy of Sciences, 978,* 289–301.

Duvernoy, H. M. (1991). *The human brain: Surface, blood supply, and three-dimensional sectional anatomy*. New York: Springer.

Ehrsson, H. H. (2007). The experimental induction of out-of-body experiences. *Science, 317,* 1048–1048.

Ehrsson, H. H. (2012). The concept of body ownership and its relation to multisensory integration. In B. Stein (Ed.), *The handbook of multisensory processes*. Boston: MIT Press.

Ehrsson, H. H., Holmes, N. P., & Passingham, R. E. (2005). Touching a rubber hand: Feeling of body ownership is associated with activity in multisensory brain areas. *The Journal of Neuroscience: The Official Journal of the Society for Neuroscience, 25,* 10564–10573.

Ehrsson, H. H., Spence, C., & Passingham, R. E. (2004). That's my hand! Activity in premotor cortex reflects feeling of ownership of a limb. *Science, 305,* 875–877.

Ehrsson, H. H., Wiech, K., Weiskopf, N., Dolan, R. J., & Passingham, R. E. (2007). Threatening a rubber hand that you feel is yours elicits a cortical anxiety response. *Proceedings of the National Academy of Sciences, U.S.A., 104,* 9828–9833.

Flor, H., Nikolajsen, L., & Jensen, T. S. (2006). Phantom limb pain: A case of maladaptive CNS plasticity? *Nature Reviews Neuroscience, 7,* 873–881.

Friston, K., Buechel, C., Fink, G., Morris, J., Rolls, E., & Dolan, R. (1997). Psychophysiological and modulatory interactions in neuroimaging. *Neuroimage, 6,* 218–229.

Gentile, G., Petkova, V. I., & Ehrsson, H. H. (2011). Integration of visual and tactile signals from the hand in the human brain: An fMRI study. *Journal of Neurophysiology, 105,* 910–922.

Graziano, M., & Botvinick, M. (2002). How the brain represents the body: Insights from neurophysiology and psychology. In W. Prinz & B. Hommel (Eds.), *Common mechanisms in perception and action: Attention and performance* (Vol. 19, pp. 136–157).

Graziano, M. S. A. (1999). Where is my arm? The relative role of vision and proprioception in the neuronal representation of limb position. *Proceedings of the National Academy of Sciences, U.S.A., 96,* 10418–10421.

Graziano, M. S. A. (2000). Coding the location of the arm by sight. *Science, 290,* 1782–1786.

Graziano, M. S. A., & Cooke, D. F. (2006). Parieto-frontal interactions, personal space, and defensive behavior. *Neuropsychologia, 44,* 2621–2635.

Graziano, M. S. A., Hu, X. T., & Gross, C. G. (1997a). Visuospatial properties of ventral premotor cortex. *Journal of Neurophysiology, 77,* 2268–2292.

Graziano, M. S. A., Hu, X. T., & Gross, C. G. (1997b). Coding the locations of objects in the dark. *Science, 277,* 239–241.

Guterstam, A., & Ehrsson, H. H. (2012). Disowning one's seen real body during an out-of-body illusion. *Consciousness and Cognition, 21,* 1037–1042.

Guterstam, A., Petkova, V. I., & Ehrsson, H. H. (2011). The illusion of owning a third arm. *PloS One, 6,* e17208.

Haans, A., IJsselsteijn, W. A., & De Kort, Y. A. W. (2008). The effect of similarities in skin texture and hand shape on perceived ownership of a fake limb. *Body Image, 5,* 389–394.

Hagura, N., Takei, T., Hirose, S., Aramaki, Y., Matsumura, M., Sadato, N., et al. (2007). Activity in the posterior parietal cortex mediates visual dominance over kinesthesia. *The Journal of Neuroscience, 27,* 7047–7053.

Hohwy, J., & Paton, B. (2010). Explaining away the body: Experiences of supernaturally caused touch and touch on non-hand objects within the rubber hand illusion. *PLoS ONE, 5,* e9416.

Holmes, N. P., & Spence, C. (2005). Multisensory integration: Space, time and superadditivity. *Current Biology, 15,* R762–R764.

IJsselsteijn, W. A., De Kort, Y. A. W., & Haans, A. (2006). Is this my hand I see before me? The rubber hand illusion in reality, virtual reality, and mixed reality. *Presence: Teleoperators and Virtual Environments, 15,* 455–464.
Ito, M. (2000). Mechanisms of motor learning in the cerebellum. *Brain Research, 886,* 237–245.
Kalckert, A., & Ehrsson, H. H. (2012). Moving a rubber hand that feels like your own: A dissociation of ownership and agency. *Frontiers in Human Neuroscience, 6.*
Lackner, J. R., & Taublieb, A. B. (1984). Influence of vision on vibration-induced illusions of limb movement. *Experimental Neurology, 85,* 97–106.
Làdavas, E., & Farnè, A. (2004). Visuotactile representation of near-the-body space. *Journal of Physiology, Paris, 98,* 161–170.
Lenggenhager, B., Tadi, T., Metzinger, T., & Blanke, O. (2007). Video ergo sum: Manipulating bodily self-consciousness. *Science, 317,* 1096–1099.
Lewis, M., & Brooks-Gunn, J. (1979). *Social cognition and the acquisition of self*. New York: Plenum.
Lloyd, D. M. (2007). Spatial limits on referred touch to an alien limb may reflect boundaries of visuotactile peripersonal space surrounding the hand. *Brain and Cognition, 64,* 104–109.
Lloyd, D. M., Shore, D. I., Spence, C., & Calvert, G. A. (2003). Multisensory representation of limb position in human premotor cortex. *Nature Neuroscience, 6,* 17–18.
Logothetis, N. K., Pauls, J., Augath, M., Trinath, T., & Oeltermann, A. (2001). Neurophysiological investigation of the basis of the fMRI signal. *Nature, 412,* 150–157.
Makin, T. R., Holmes, N. P., & Ehrsson, H. H. (2008). On the other hand: Dummy hands and peripersonal space. *Behavioural Brain Research, 191,* 1–10.
Makin, T. R., Holmes, N. P., & Zohary, E. (2007). Is that near my hand? Multisensory representation of peripersonal space in human intraparietal sulcus. *The Journal of Neuroscience, 27,* 731–740.
Maravita, A., & Iriki, A. (2004). Tools for the body (schema). *Trends in Cognitive Sciences, 8,* 79–86.
Maravita, A., Spence, C., & Driver, J. (2003). Multisensory integration and the body schema: Close to hand and within reach. *Current Biology, 13,* R531–R539.
Marconi, B., Genovesio, A., Battaglia-Mayer, A., Ferraina, S., Squatrito, S., Molinari, M., et al. (2001). Eye-hand coordination during reaching. I. Anatomical relationships between parietal and frontal cortex. *Cerebral Cortex, 11,* 513–527.
Mesulam, M. M., & Mufson, E. J. (1982). Insula of the old world monkey. III: Efferent cortical output and comments on function. *The Journal of Comparative Neurology, 212,* 38–52.
Miall, R. C., Weir, D. J., Wolpert, D. M., & Stein, J. F. (1993). Is the cerebellum a Smith predictor? *Journal of Motor Behavior, 25,* 203–216.
Miyazaki, M., Hirashima, M., & Nozaki, D. (2010). The "cutaneous rabbit" hopping out of the body. *The Journal of Neuroscience, 30,* 1856–1860.
Moseley, G. L., Gallace, A., & Spence, C. (2012). Bodily illusions in health and disease: Physiological and clinical perspectives and the concept of a cortical "body matrix." *Neuroscience & Biobehavioral Reviews, 36,* 34–46.
Moseley, G. L., Olthof, N., Venema, A., Don, S., Wijers, M., Gallace, A., et al. (2008). Psychologically induced cooling of a specific body part caused by the illusory ownership of an artificial counterpart. *Proceedings of the National Academy of Sciences, U.S.A., 105,* 13169–13173.
Myers, A., & Sowden, P. T. (2008). Your hand or mine? The extrastriate body area. *Neuroimage, 42,* 1669–1677.
Obayashi, S., Tanaka, M., & Iriki, A. (2000). Subjective image of invisible hand coded by monkey intraparietal neurons. *NeuroReport, 11,* 3499–3505.
Orioli, P. J., & Strick, P. L. (1989). Cerebellar connections with the motor cortex and the arcuate premotor area: An analysis employing retrograde transneuronal transport of WGA-HRP. *The Journal of Comparative Neurology, 288,* 612–626.
Orlov, T., Makin, T. R., & Zohary, E. (2010). Topographic representation of the human body in the occipitotemporal cortex. *Neuron, 68,* 586–600.
Passingham, R. (1993). *The frontal lobes and voluntary action*. Oxford: Oxford University Press.
Passingham, R. E., Bengtsson, S. L., & Lau, H. C. (2010). Medial frontal cortex: From self-generated action to reflection on one's own performance. *Trends in Cognitive Sciences, 14,* 16–21.
Petkova, V. I., Björnsdotter, M., Gentile, G., Jonsson, T., Li, T.-Q., & Ehrsson, H. H. (2011). From part- to whole-body ownership in the multisensory brain. *Current Biology, 21,* 1118–1122.
Petkova, V. I., & Ehrsson, H. H. (2008). If I were you: Perceptual illusion of body swapping. *PloS One, 3,* e3832.
Petkova, V. I., & Ehrsson, H. H. (2009). When right feels left: Referral of touch and ownership between the hands. *PLoS ONE, 4,* e6933.
Ramachandran, V. S., & Hirstein, W. (1998). The perception of phantom limbs. The D. O. Hebb lecture. *Brain: A Journal of Neurology, 121,* 1603–1630.
Rizzolatti, G., Luppino, G., & Matelli, M. (1998). The organization of the cortical motor system: New concepts. *Electroencephalography and Clinical Neurophysiology, 106,* 283–296.
Rizzolatti, G., Scandolara, C., Matelli, M., & Gentilucci, M. (1981). Afferent properties of periarcuate neurons in macaque monkeys. II. Visual responses. *Behavioural Brain Research, 2,* 147–163.
Rochat, P. (1998). Self-perception and action in infancy. *Experimental Brain Research. Experimentelle Hirnforschung. Expérimentation Cérébrale, 123,* 102–109.
Rohde, M., Di Luca, M., & Ernst, M. O. (2011). The rubber hand illusion: Feeling of ownership and proprioceptive drift do not go hand in hand. *PLoS ONE, 6,* e21659.
Schmalzl, L., & Ehrsson, H. H. (2011). Experimental induction of a perceived "telescoped" limb using a full-body illusion. *Frontiers in Human Neuroscience, 5,* 34.
Stein, B. E., & Stanford, T. R. (2008). Multisensory integration: Current issues from the perspective of the single neuron. *Nature Reviews Neuroscience, 9,* 255–266.
Tsakiris, M. (2010). My body in the brain: A neurocognitive model of body-ownership. *Neuropsychologia, 48,* 703–712.
Tsakiris, M., Carpenter, L., James, D., & Fotopoulou, A. (2010). Hands only illusion: Multisensory integration elicits sense of ownership for body parts but not for non-corporeal objects. *Experimental Brain Research, 204,* 343–352.
Tsakiris, M., & Haggard, P. (2005). The rubber hand illusion revisited: Visuotactile integration and self-attribution. *Journal of Experimental Psychology: Human Perception and Performance, 31,* 80–91.
Tsakiris, M., Hesse, M. D., Boy, C., Haggard, P., & Fink, G. R. (2007). Neural signatures of body ownership: A sensory network for bodily self-consciousness. *Cerebral Cortex (New York, N.Y.: 1991), 17,* 2235–2244.
Tsakiris, M., Prabhu, G., & Haggard, P. (2006). Having a body versus moving your body: How agency structures body-ownership. *Consciousness and Cognition, 15,* 423–432.

Van Beers, R. J., Sittig, A. C., & Denier van der Gon, J. J. (1996). How humans combine simultaneous proprioceptive and visual position information. *Experimental Brain Research, 111,* 253–261.
Van den Bos, E., & Jeannerod, M. (2002). Sense of body and sense of action both contribute to self-recognition. *Cognition, 85,* 177–187.
Viswanathan, S., Fritz, C., & Grafton, S. T. (2012). Telling the right hand from the left hand multisensory integration, not motor imagery, solves the problem. *Psychological Science, 23,* 598–607.
Walsh, L. D., Moseley, G. L., Taylor, J. L., & Gandevia, S. C. (2011). Proprioceptive signals contribute to the sense of body ownership. *The Journal of Physiology, 589,* 3009–3021.
Welch, R. B., & Warren, D. H. (1986). Intersensory interactions. In L. Kaufman & J. P. Thomas (Eds.), *Handbook of perception and human performance*. New York: Wiley.
Welch, R. B., Widawski, M. H., Harrington, J., & Warren, D. H. (1979). An examination of the relationship between visual capture and prism adaptation. *Perception & Psychophysics, 25,* 126–132.